Analytical Methods

ROYAL SOCIETY OF CHEMISTRY

CRITICAL REVIEW

View Article Online
View Journal | View Issue

Cite this: *Anal. Methods*, 2025, **17**, 4697

Advancing food safety and quality assessment: a comprehensive review of non-destructive analytical technologies

Yuerong Feng, Xinai Zhang, * Jiaqian Liu, Zhecong Yuan, Shujie Gao and Jiyong Shi *

Non-destructive analytical technologies have emerged as transformative tools for advancing food safety and quality assessment, addressing critical challenges posed by chemical contaminants, microbial pathogens, and adulterants in global food supply chains. This review critically evaluates five advanced technologies—hyperspectral imaging (HSI), electrochemical sensing, infrared spectroscopy, surface-enhanced Raman scattering (SERS), and fluorescence sensing—highlighting their operational principles, validation milestones, and applications across diverse food matrices. Despite remarkable progress, several methodological gaps remain, including signal instability in heterogeneous samples, limited algorithm generalizability, and the lack of standardized validation protocols. Furthermore, real-time field deployment faces challenges such as sensor miniaturization, environmental robustness, and cost constraints. Emerging hybrid platforms such as HSI-SERS and electrochemical-fluorescence systems demonstrate promising synergistic advantages, offering enhanced specificity and multiplexing capabilities. Future directions emphasize integration of AI-driven analytics, IoT-enabled portable devices, and novel functional materials to address existing limitations. By bridging technological innovation with regulatory needs, this review underscores the potential of non-destructive technologies to build scalable, sustainable food safety solutions.

Received 17th April 2025
Accepted 20th May 2025

DOI: 10.1039/d5ay00647c

rsc.li/methods

1 Introduction

Globalization and shifting consumption patterns have amplified food safety risks, positioning it as a critical challenge to public health and economic stability.[1,2] Recent decades have witnessed recurrent food safety incidents involving chemical contaminants, unauthorized additives, pathogenic microorganisms, and pesticide residues, collectively threatening consumer well-being and eroding trust in food systems.[3,4] These concerns have prompted substantial investments by governments, industries, and research institutions in advanced quality control frameworks spanning the production, processing, and distribution stages.[5,6]

Traditional food safety evaluation predominantly relies on destructive analytical techniques such as chromatography, culture-based microbiological assays, and physicochemical testing.[7] While these methods provide benchmark accuracy, they present inherent limitations: extensive sample preparation, analysis durations ranging from several hours to days, high operational costs, and dependence on skilled personnel.[8,9] Moreover, destructive sampling precludes real-time monitoring and introduces representativeness errors, particularly in heterogeneous food matrices.[10] These constraints underscore the urgent need for rapid, non-invasive analytical solutions capable of *in situ* implementation without compromising analytical rigor.[11]

Recent advances in optical and electrochemical sensing technologies present paradigm-shifting opportunities. Hyperspectral imaging (HSI) synergizes spatial and spectral data across ultraviolet to near-infrared wavelengths (250–2500 nm), enabling non-contact detection of surface contaminants, compositional gradients, and structural defects in agricultural products.[12] Electrochemical biosensors achieve parts-per-billion sensitivity for heavy metals, antibiotics, and microbial toxins through tailored bioreceptor-functionalized electrodes, offering portable alternatives to laboratory-based instrumentation.[13] Infrared spectroscopy technology, especially near-infrared spectroscopy (NIR) and Fourier transform transmission infrared spectroscopy (FTIR), has demonstrated significant potential in food quality control, composition analysis, and processing monitoring.[14] Surface-enhanced Raman spectroscopy (SERS) technology provides specific chemical fingerprint information by exciting molecular vibrational modes, enabling precise analysis of trace components in food. It is especially suitable for detecting organic compounds in complex food matrices.[15] Fluorescence sensing technology utilizes the excitation and emission properties of substances for signal output, enabling the detection of various components in food (Table 1).[16]

School of Food and Biological Engineering, Jiangsu University, Zhenjiang 212013, P. R. China. E-mail: zhangxinai@ujs.edu.cn; shi_jiyong@ujs.edu.cn

Table 1 The principles of advanced technologies and their test objects, as well as their applications in food

Technical term	Detection principle	Target object	Applications in food
HSI	By capturing a wide spectrum of light across different wavelengths, enabling the identification of chemical composition and quality based on spectral signatures	Food freshness, moisture content, food contaminants, soluble solids content, volatile basic nitrogen, pesticide residues, heavy metals, mycotoxins	Grapes, pork, egg, citrus, lettuce leaves, wolfberry fruits, corn leaves, cantaloupes, sorghum, rapeseed leaves, rice, tomato leaves, corn starch, wheat
Electrochemical sensing	By measuring the electrical signals generated from the interaction between food components and an electrode, providing insights into chemical composition or contaminants	Mycotoxins, heavy metal ions, pesticide residues	Milk, rice, shiitake mushrooms, dairy products, ganoderma lucidum, pomegranate
Infrared spectroscopy	By analyzing the absorption of infrared light at different wavelengths, revealing information about the molecular structure and composition of the food	Soluble solid content, volatile basic nitrogen, mycotoxins, food freshness, heavy metal, pesticide residues	Corn, apples, eggs, watermelon seeds, tea leaves, wheat grains and flour, corn oil, crayfish, aristichthys nobilis, pork, peanuts, rice, strawberries, cabbage
SERS	By utilizing surface plasmon resonance to amplify Raman signals, allowing for highly sensitive identification of chemical components and contaminants at the molecular level	Toxins, pesticide residues	Tea leaves, apples, corn oil, palm oil, beef, rice, pears, bananas, citrus
Fluorescence sensing	By measuring the fluorescence emitted when food components absorb specific wavelengths of light, providing insights into their chemical properties and detecting contaminants	Pesticide residues, neurotoxin, carcinogen acrylamide, heavy metals, mycotoxins	Rice, cabbage, milk, pork, amaranth

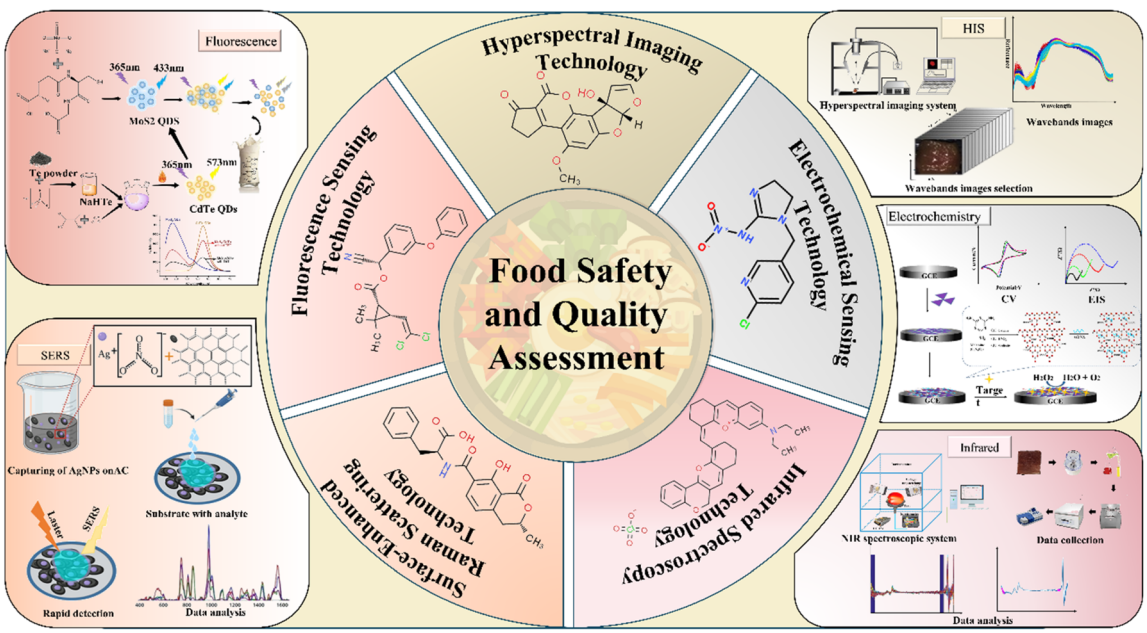

Scheme 1 A comprehensive summary of the principles and applications of non-destructive analytical technologies.

This review critically examines the mechanisms, validation benchmarks, and practical challenges of non-destructive technologies, establishing structure–property-application relationships for diverse food hazards (Scheme 1). We propose a decision-making framework for technology selection tailored to specific safety scenarios and highlight synergistic

opportunities between AI-driven spectral analysis and blockchain-enabled traceability systems. By integrating multidisciplinary advancements, this work aims to accelerate the translation of analytical innovations into scalable, environmentally sustainable food safety infrastructure, ensuring compliance with global standards while minimizing economic and ecological burdens.

2 HSI in food safety and quality assessment

2.1 Fundamental principles of HSI

HSI is a powerful analytical technique that captures a wide spectrum of light from an object, providing detailed spectral information across multiple wavelengths.[17] This technology is particularly valuable in food quality assessment, as it allows for non-destructive evaluation of various attributes, including the freshness, contamination, and quality of food.[18] HSI operates by collecting data from numerous continuous spectral bands, typically in the visible to near-infrared range (400–1000 nm). A typical HSI system comprises a spectrometer, a camera with lenses, lighting devices, a motor-driven movable platform, and a computer with image acquisition software (Fig. 1a).[19] Each pixel in a hyperspectral image corresponds to a spectrum representing the reflected light. This spectral information reveals insights into the chemical composition and physical properties of the analyzed food sample.[20] For example, the reflectance spectrum may be influenced by factors such as moisture content, sugar levels, and the presence of contaminants or defects.

The acquisition of hyperspectral data requires the use of specialized cameras capable of capturing images across a wide range of wavelengths.[21] Once the images are acquired, various data processing techniques are applied to extract meaningful information. Common techniques include the use of standard normal variate (SNV) for spectral data normalization and variable selection methods, such as iteratively retained informative variables. These preprocessing steps are crucial for improving the accuracy and reliability of subsequent analysis. The workflow typically also involves various chemometric methods (Fig. 1b), which help interpret spectral information. For example, Support Vector Regression (SVR) has been widely used to predict specific quality indicators, the total soluble solids (TSS)in grapes[22] and total volatile basic nitrogen (TVB-N) in pork.[23] These models use spectral data to provide a quantitative assessment of food quality, enabling fast and effective evaluations.

Recent advancements in deep learning have further enhanced the capabilities of HSI. For example, a dual-branch convolutional neural network (CNN) has been proposed to quantify pork freshness, achieving a high prediction accuracy

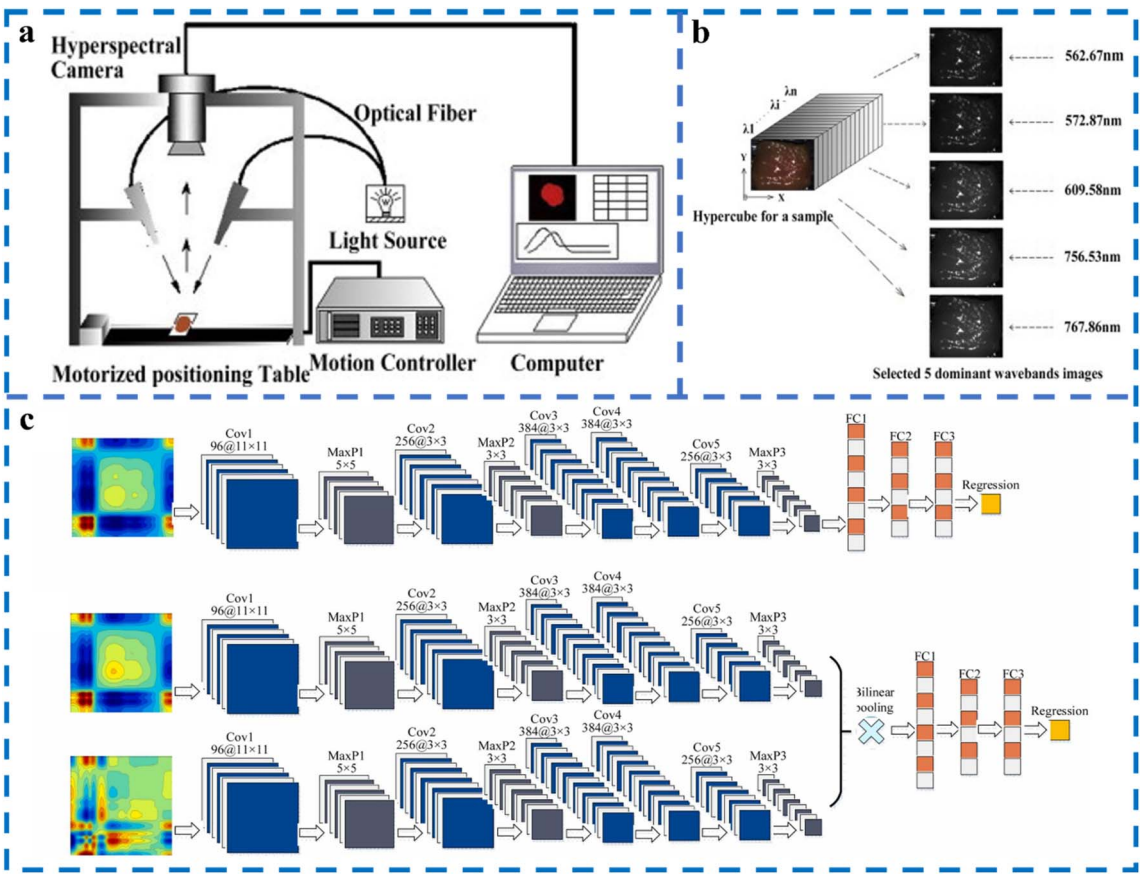

Fig. 1 (a) Hypersectral imaging system.[19] (b) Selection of feature band images from hypercube *via* synergy interval partial least squares (Si-PLS) and Genetic Algorithm (GA).[23] (c) Structure of conventional CNN and dual-branch CNN.[24]

with $R^2 = 0.9579$ (Fig. 1c).[24] This approach demonstrates how machine learning techniques can be integrated with hyperspectral data to produce better results in food quality assessment.

In conclusion, HSI represents a significant advancement in non-destructive food quality assessment. It captures detailed spectral information and, combined with sophisticated data analysis techniques, provides a powerful framework for evaluating various quality attributes in food. Ongoing research in this field continues to expand its applications, paving the way for more precise, efficient, and scalable food safety and quality control strategies.

2.2 Applications in food quality monitoring

2.2.1 Real-time freshness and spoilage evaluation. HSI has become a powerful tool for assessing the freshness and quality of various foods. In the prediction of egg freshness, Yao *et al.* demonstrated the effectiveness of HSI in detecting egg freshness, scattered yolks, and eggshell cracks. By utilizing a quantitative model based on Extreme Gradient Boosting (XGBoost), they achieved a coefficient of determination (R^2) of 0.91 in predicting egg freshness, indicating high accuracy in non-destructive assessment.[25] A study employed HSI combined with chemometric methods to achieve nondestructive and rapid classification of egg freshness. By applying preprocessing, characteristic wavelength selection, and a support vector machine (SVM) model optimized using a GA, the IRIV-GA-SVM model achieved classification accuracies of 99.29% and 97.87% for the training and testing sets, respectively.[26] Yao *et al.* utilized HSI combined with outlier elimination methods based on leverage and Cook's distance to achieve nondestructive detection of the Haugh unit of eggs. Characteristic wavelengths within the range of 530–800 nm were selected using the Successive Projections Algorithm (SPA) and Bootstrapping Soft Shrinkage (BOSS) algorithm, and a Harris Hawks Optimization-Support Vector Regression (HHO-SVR) model was developed. The results showed that the HHO-SVR model yielded the highest prediction accuracy ($R_p^2 = 0.9523$, RMSEP = 3.0423). Furthermore, validation with brown-shelled eggs confirmed the model's generalizability, highlighting the potential of hyperspectral imaging technology in egg freshness assessment.[27]

In the prediction of pork freshness, Sun *et al.* proposed a novel approach that integrates a CNN with two-dimensional correlation spectroscopy (2D-COS). By enhancing the model's predictive capability for pork TVB-N content through synchronous–asynchronous feature interaction, the method achieved high-precision detection ($R_p = 0.9579$, RMSEP = 0.8093 mg/100 g).[24] A supplementary study by Li *et al.* highlighted the importance of combining HSI with colorimetric sensors to measure TVB-N content in pork. Their novel back propagation adaptive boosting (BP-AdaBoost) algorithm achieved a prediction ratio of 2.885 and a calibration coefficient of 0.932, confirming the advantages of combining multiple sensing technologies.[23] Tang *et al.* integrated hyperspectral information with image texture information to analyze the quality characteristics of a large number of pork samples. After adding texture information, the prediction accuracy for all attributes of the pork samples improved by varying degrees, increasing from the original 1.5% to 16.4%.[28] Cheng *et al.* utilized visible near-infrared hyperspectral imaging (vis-NIR HSI) and fluorescence hyperspectral imaging (F-HSI) technologies combined with a Gaussian process regression (GPR) model to achieve non-destructive detection of lipid oxidation in frozen pork. The F-HSI model demonstrated slightly superior predictive accuracy ($R_p^2 = 0.9726$, RMSEP = 0.0182 mg kg^{-1}). By generating pseudo-color distribution maps of TBARS values utilizing the F-HSI model, the feasibility of F-HSI for quantitative monitoring and visualization of lipid oxidation in pork was validated (Fig. 2a).[29] These studies demonstrate that HSI can effectively evaluate pork freshness. In addition to freshness testing, HSI has also been successfully used to monitor other quality attributes.

In food quality assessment, Dong *et al.* proposed a single-threshold segmentation strategy based on HSI combined with principal component analysis (PCA) of characteristic wavelengths and the B-spline lighting correction method, achieving high-precision detection of thrips defects on green-peel citrus with an accuracy of 96.5%.[30] In addition, non-destructive assay of lettuce moisture content has been explored using HSI, demonstrating the versatility in the quality assessment of different foods.[31] Hu *et al.* pioneered the integration of HSI with machine learning methods, optimizing Vis-NIR band data and utilizing an random forest-partial least squares regression (RF-PLSR) model to achieve rapid, non-destructive evaluation and visualization of matcha quality (classification accuracy 98.10%, $R_p^2 > 0.95$).[32] Nirere *et al.* achieved non-destructive and rapid detection of sulfur-adulterated wolfberries using hyperspectral imaging technology combined with competitive adaptive reweighted sampling (CARS) feature wavelength selection and a genetic algorithm-optimized SVM model, with both training and test set accuracies reaching 100%.[33]

2.2.2. Contaminant identification in complex food matrices. HSI plays a crucial role in detecting contaminants in food. In terms of pesticide residues, Sun *et al.* adopted HSI combined with CARS and random forest-recursive feature elimination (RF-RFE) feature wavelength selection strategies. Through secondary optimization with SPA and least squares support vector regression (LSSVR) modeling, they achieved non-destructive quantitative detection of mixed pesticide residues (fenvalerate: $R_p^2 = 0.8890$, RMSEP = 0.0182; dimethoate: $R_p^2 = 0.9386$, RMSEP = 0.0077) in lettuce leaves.[34] Xiao *et al.* analyzed the residue levels in six resistant and sensitive maize varieties under two herbicide concentrations, classifying the residues into low, medium, and high categories. They developed the HerbiResNet model leveraging spectral data to predict and categorize herbicide residues in maize leaves. The experimental results demonstrated that the HerbiResNet model achieved a determination coefficient (R^2) of 0.88 for residue prediction and an accuracy of 0.87 for residue level classification on the test set, significantly outperforming traditional regression models and classical neural networks (Fig. 2b).[35] Bian *et al.* employed microfluorescence hyperspectral imaging (MF-HSI) technology combined with machine learning methods. By screening characteristic wavelengths using CARS, GA, and SPA, and integrating key color

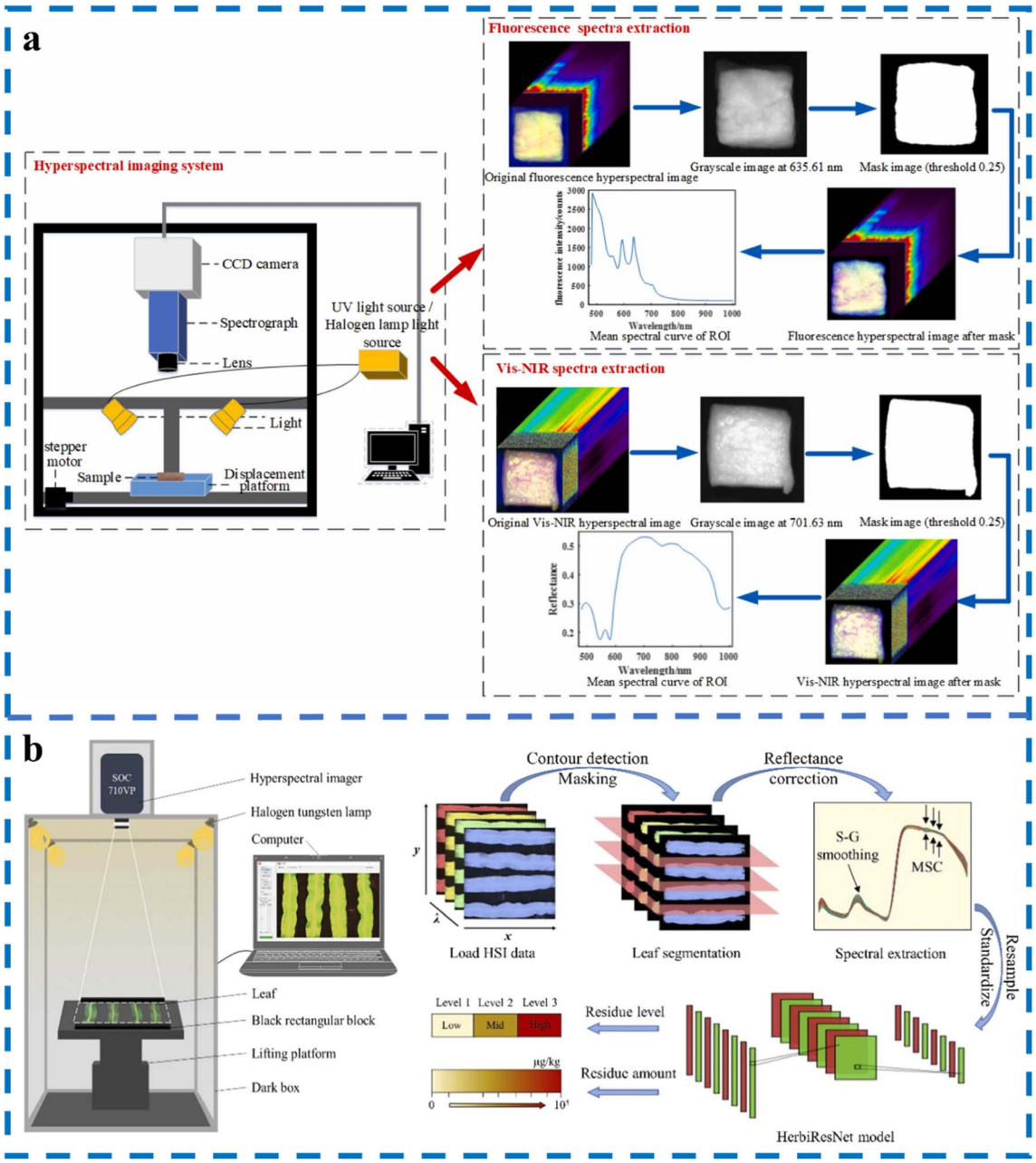

Fig. 2 Schematic diagram of the applications hyperspectral imaging technology. (a) Architecture of the F-HIS and VNIR-HSI systems for pork freshness assessment.[29] (b) Deep learning-driven herbicide residue detection system and workflow for agricultural product monitoring.[35]

features (G, B, V, L), they achieved high-precision identification of three pesticide residues, including Beta-Cypermethrin, in Hami melons. The results showed that the SPA-PLS-DA model, which fused spectral and image features, achieved a testing set accuracy of 93.48%, significantly outperforming single-spectrum models.[36] By combining HSI technology with stacked ensemble learning (SEL) models, Peng *et al.* developed a rapid method for analyzing pesticide residues in sorghum, with RMSEP and R^2 values of 0.6940 mg kg^{-1} and 0.9798, respectively.[37] These studies demonstrate the assay effectiveness of HSI in pesticide residue.

In the field of heavy metals, Cao *et al.* developed a method based on visible-near infrared hyperspectral technology, utilizing an improved random frog algorithm (MRF) combined with a Harris Hawks Optimizer (HHO)-optimized support vector regression model (MRF-HHO-SVR), achieving non-destructive and high-precision detection of Pb content in rape leaves (R^2 = 0.9431, RMSEP = 0.1645 mg kg^{-1}).[38] Zhou *et al.* proposed a deep learning framework based on wavelet transform (WT) and stacked convolutional autoencoder (SCAE). Through multi-scale decomposition and deep feature learning, they achieved high-precision detection of compound heavy metals in lettuce leaves (Cd: R_p^2 = 0.9319, RMSEP = 0.04988 mg kg^{-1}; Pb: R_p^2 = 0.9418, RMSEP = 0.04123 mg kg^{-1}).[39] Sun *et al.* achieved non-destructive detection of lead pollution levels in lettuce leaves by combining

HSI with a deep belief network (DBN) model. Under four lead stress gradients (0–200 mg L^{-1}), the DBN model achieved 100% accuracy on the training set and 96.67% on the test set, with the separability of model features validated through t-SNE visualization.[40] These studies indicated the effectiveness of HSI in detecting heavy metals.

In the field of mycotoxins detection, Sunli *et al.* achieved non-destructive detection of the total number of mold colonies in rice by integrating HSI with a Gray Wolf Optimization (GWO)-optimized support vector regression (GWO-SVR) model, achieving determination coefficients of 0.9621 for the calibration set and 0.9511 for the prediction set.[41] Zhang *et al.* established a recognition model for different levels of tomato leaf blight using backpropagation neural networks (BPNN) combined with NIR-HSI, terahertz absorbance, and power spectra, achieving recognition rates of 95%, 96.67%, and 95%, respectively. This highlighted the multifunctionality of HSI in detecting various contaminants and diseases.[42] Kim *et al.* integrated visible-near-infrared (VNIR), short-wave infrared (SWIR), and fluorescence hyperspectral imaging technologies, employing SVM and partial least squares-discriminant analysis (PLS-DA) models to achieve efficient screening of aflatoxin and fumonisin contamination, both individually and co-occurring, in maize. Results demonstrated that the SWIR-SVM model

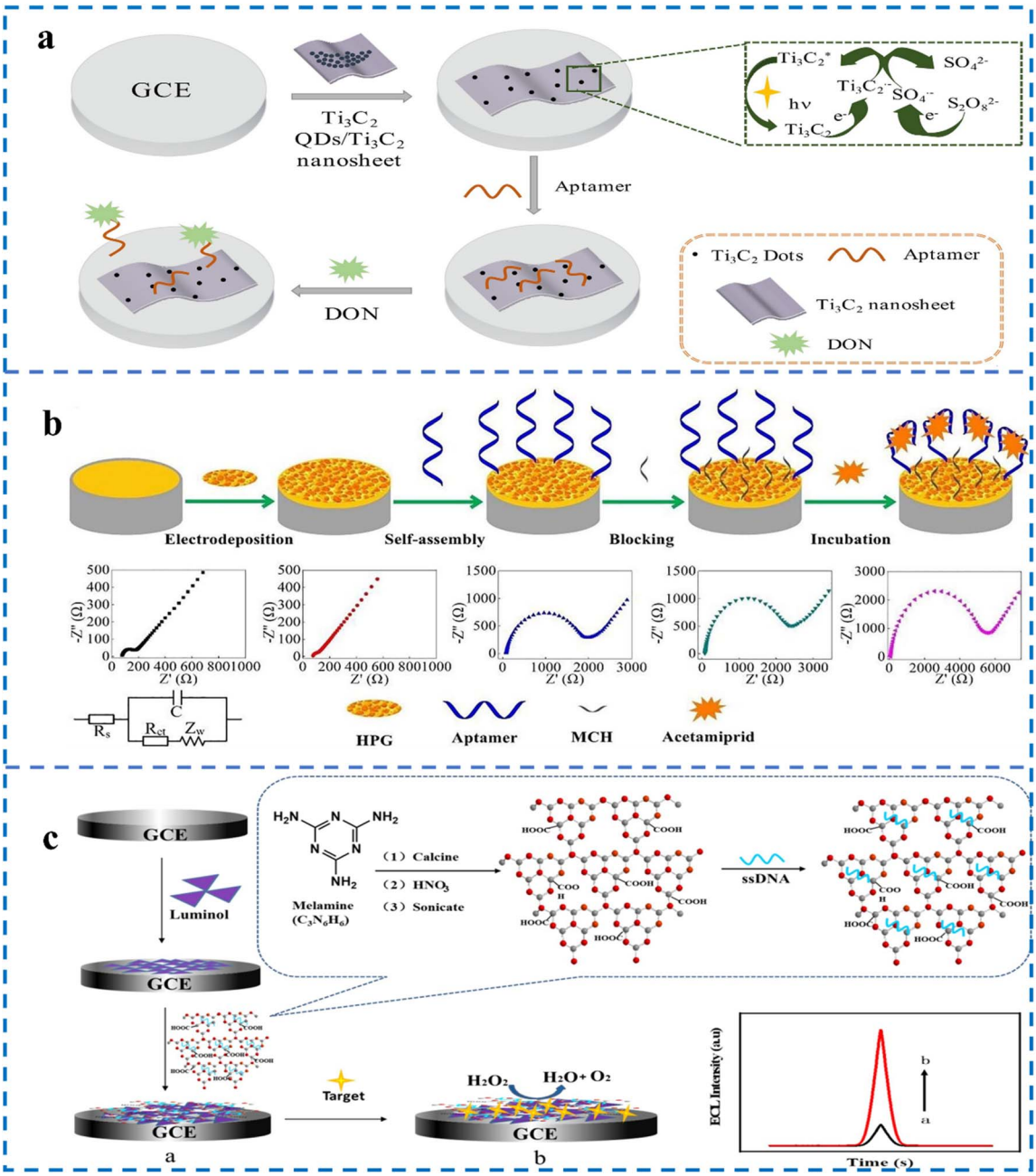

Fig. 3 Principle of electrochemical sensing technology. (a) Schematic of ECL aptamer sensor based on TDTN for detecting DON.[51] (b) Aptamer sensor based on ABA/HPG/AuE for detecting acetamiprid.[52] (c) Principle of the ECL sensor based on ssDNA/g-C_3N_4NS for detecting H_2O_2.[53]

achieved the highest classification accuracy (95.7%), significantly outperforming fluorescence (89.1%) and VNIR (71.7%) models.[43] Teixido-Orries *et al.* applied NIR-HSI technology for the first time to detect T-2/HT-2 toxins in 119 naturally contaminated oat samples. By combining PLS regression models and classification algorithms, they found that unground samples with SNV combined with first-derivative pretreatment achieved the best prediction performance (R^2 = 0.64, RMSECV = 157.80 μg kg^{-1}). The study confirmed that NIR-HSI, combined with characteristic wavelengths (1038, 1110, and 1393 nm), enables rapid and non-destructive screening of oat toxins, offering a feasible alternative to traditional chemical detection methods, though further validation of the model's generalization ability is needed.[44] Wang *et al.* also utilized NIR-HSI to predict DON content in wheat. These studies all demonstrated strong prediction coefficients, proving the effectiveness of HSI in the detection of mycotoxins.[45]

3 Electrochemical sensing for food safety analysis

3.1 Design and fabrication of electrochemical sensors

Electrochemical sensors are widely used analytical tools in the field of food safety monitoring.[46] Their fundamental principle is to detect target analytes by measuring changes in electrochemical parameters, such as current, voltage, or conductivity.[47] A typical electrochemical sensor consists of a working electrode, a reference electrode, and an auxiliary electrode. By monitoring the current generated during the reaction, the concentration of the target substance can be determined.[48] Additionally, biomolecular recognition elements can be modified onto the sensing interface for selective recognition.[49] Common electrochemical measurements include potentiometry, cyclic voltammetry (CV), electrochemical impedance spectroscopy (EIS), square wave voltammetry (SWV), and differential pulse voltammetry (DPV).[50]

Regarding food assay, key concepts of electrochemical technology include sensitivity, selectivity, and detection limit (LOD). Sensitivity refers to the relationship between the response intensity and target concentration. A highly sensitive sensor with high sensitivity can reliably detect the target substance at low level. For example, studies have shown that an electrochemiluminescence (ECL) sensor based on Ti_3C_2 points and Ti_3C_2 nanosheets can detect deoxynivalenol (DON) with a detection range of 0.001–20 ng mL^{-1} and a LOD of 0.3 pg mL^{-1} (Fig. 3a).[51] This demonstrates the sensor's capability to accurately identify DON even at extremely low concentrations.

Selectivity refers to the ability of a sensor to accurately identify target substance in the presence of interfering substances. Improving selectivity is typically achieved through specific modifying materials or biomolecular recognition elements. For example, electrochemical sensors using functionalized gold nanoparticles and specific aptamers have shown high selectivity and sensitivity in detecting pesticide residues in food (Fig. 3b).[52] This enables effective discrimination of the target analyte from background interference in complex matrices such as fruits, vegetables, and meats.

The LOD refers to the lowest concentration at which the sensor can reliably detect a substance. This parameter is particularly important for food safety monitoring, as many harmful substances are present in extremely low concentrations in food. For example, a non-enzymatic ECL sensor based on single-stranded DNA (ssDNA) and graphene carbon nitride nanosheets (g-C_3N_4NS) hybrids has achieved a LOD as low as 33 aM, which is much lower than most of the reported methods (Fig. 3c).[53] Such a low LOD allows the sensor to achieve fast and accurate assay in food safety monitoring.

Regarding sensor construction, several studies have exploited composite materials to enhance the performance of electrochemical sensors. For example, Wang *et al.* utilized amino-functionalized metal–organic frameworks (UiO-66-NH_2) combined with multi-walled carbon nanotubes (MWCNTs) to fabricate a high-performance electrochemical sensor for lead ion detection, demonstrating excellent sensitivity and a wide linear range.[54] Liu *et al.* constructed a competitive dual-mode aptamer sensor for the detection of acetamiprid (ACE) residues in vegetables. By employing 3,5-dicarboxyphenylboronic acid (5-bop) as the ligand, a bimetallic RuZn-based metal–organic framework (RuZn-MOF) was synthesized through a hydrothermal approach, which facilitated highly sensitive dual-mode detection of ACE *via* ECL and electrochemical (EC) techniques.[55] Zhang *et al.*, based on functionalized carbon nanotubes loaded with thiosulfo-mannose dimers, designed a competitive recognition principle to create an electrochemical biosensor.[56] Shu *et al.* synthesized an iron-rich FeCoNi-MOF using a one-step hydrothermal pattern for *in situ* modification of a nickel foam working electrode, enabling high-sensitivity detection of imidacloprid (IMI).[57] These studies demonstrate that the use of composite materials consistently improved sensor performance. Although the construction methods of the sensors share similarities, the research results exhibit significant differences, which may stem from variations in material selection, sensor design, and signal amplification mechanisms.

3.2 Targeted detection of food hazards

3.2.1. Detection of mycotoxins. The application of electrochemical sensing toward mycotoxins demonstrates their superior sensitivity and wide detection range. According to research, Kaur *et al.* designed a highly selective and sensitive electrochemical sensor for detecting aflatoxins (AFM) by modifying a screen-printed carbon electrode with functional nanocomposites of molybdenum disulfide (MoS_2) quantum dots (QDs) and zirconium-based metal–organic frameworks (MOF), that is, UiO-66-NH_2. The results showed that the calibration curve for AFM exhibited a quantifiable lower limit of 0.06 ng mL^{-1} within a concentration range of 0.2–10 ng mL^{-1}.[58] Liu *et al.* used high-affinity aptamers to measure mycotoxins, and also found that aptamers with different sequences exhibited varying sensitivities in electrochemical assays. Among them, the A22 aptamer showed a good linear range and LOD in the analysis of apple products (such as juice and puree), further

validating the broad application of electrochemical sensors in food safety detection.[59] In addition, Jiang *et al.* used a dual-signal strategy with Co-MOF and toluidine blue tags to detect ochratoxin A (OTA). The results showed that the LOD was as low as 0.31 fg mL^{-1} within a linear range of 1–50 ng mL^{-1}.[60] These studies indicate that electrochemical sensors are effective and widely applicable in the detection of mycotoxins.

3.2.2. Detection of heavy metal ions. Research on the detection of heavy metal ions in food based on electrochemical sensing technology has been increasingly growing. For example, Hormozi Jangi *et al.* developed a highly sensitive and selective strategy for the detection of Cd^{2+}. The study first synthesized sodium aluminate nanostructures *via* a sol–gel method combined with a green synthesis route. These nanostructures were then utilized to fabricate a modified nanostructured sensor. The performance of the sensor was evaluated using DPV, achieving a remarkable LOD of 1.10 nM for Cd^{2+}.[61] Zhang *et al.* developed a light-addressable potentiometric sensor (LAPS) to detect Cd^{2+} in rice.[62] Xu *et al.* designed a polymer-dot (Pdots)-based aggregation-induced ECL sensing toward Cd^{2+}. This sensor demonstrated excellent capabilities for Cd^{2+} in ganoderma lucidum, with a LOD as low as 0.006 ppb.[63] In addition, Zhang *et al.* developed a reagent-free, one-step electrochemical aptamer sensor for detecting Hg^{2+} in dairy products.[64] Huang *et al.* utilized the mimic catalytic activity of porphyrin-encapsulated MOF (PorMOF) as a signal probe to prepare an electrochemical aptamer sensor, successfully detecting Ag^{+} in shiitake mushrooms.[65] Lu *et al.* designed an electrochemical sensor for detecting Pb^{2+} in pomegranate based on a DNAzyme receptor and Fenton-like MOF.[66] These studies demonstrate high selectivity and good assay performance, further emphasizing the importance of electrochemical sensing toward heavy metal ions.

3.2.3. Detection of pesticide residues. Electrochemical sensors show broad application potential in detecting pesticide residues. For example, a non-precious metal-based photoelectrochemical (PEC) sensor has been developed for analyzing chlorpyrifos, exhibiting ultra-high sensitivity and selectivity in fruits and vegetables. The detection range is from 1×10^{-3} to 1 ng L^{-1}, with a LOD of 0.33 pg L^{-1}, showing excellent repeatability and stability.[67] Notably, Zhao *et al.* have shown that graphene nanoribbons (DGNR), as a novel electrode material, also exhibit excellent performance in detecting methyl parathion (MP), with a LOD of 4.3 nM and a linear range of 0.01 to 25.0 μM, further expanding the application potential of electrochemical sensors in pesticide residue detection.[68] Devi *et al.* designed an electrochemical sensor for detecting malathion using a novel B-CuO/g-C_3N_4 ternary nanocomposite, with a LOD as low as 1.2 pg mL^{-1}.[69] Rashed *et al.* used silver nanoparticles (AgNPs) onto mesoporous carbon and naturally extracted hematite (Ag@Meso-C/Hematite Ore) to sensitively and selectively measure imidacloprid (IMC), with a LOD of 0.257 μM.[70] These studies demonstrate that electrochemical sensors possess high specificity and good capability in the detection of pesticide residues.

4 Infrared spectroscopy in food safety and quality assessment

4.1 Theoretical basis and spectral data modeling

Infrared spectroscopy is an analytical method based on the principle of interaction between substances and infrared radiation.[71] It provides information about molecular structure and chemical composition by measuring the infrared spectrum absorbed by a sample.[72] Commonly used infrared spectroscopy techniques include FTIR and NIR.

NIR spectroscopy detects overtone and combination bands of molecular vibrations in the wavelength range of 800–2500 nm, particularly those associated with C–H, N–H, and O–H bonds.[73] Owing to its rapid analysis and minimal sample preparation requirements, NIR is widely adopted for real-time food composition analysis and quality control. In contrast, FTIR primarily operates in the mid-infrared region (2.5–25 μm, 4000–400 cm^{-1}), where fundamental molecular vibrations occur, enabling detailed characterization of chemical structures and environmental interactions.

As for infrared spectroscopy data analysis, the application of chemometric patterns has gradually gained attention, especially in the construction and optimization of quantitative models.[74] Partial Least Squares Regression (PLS) is one of the most commonly used chemometric methods. It enhances the predictive ability of the model by extracting the correlation between the independent and dependent variables into latent components.[75] In a study, researchers used a portable near-infrared spectrometer SVM to construct quantitative models for fumonisin B1 and B2 in corn samples.[76]

Feature variable selection is a key step in improving the predictive accuracy of infrared spectroscopy models. By reducing irrelevant or redundant variables, the performance and interpretability of the model can be enhanced.[77] For example, CARS is an effective feature selection that chooses the optimal variables through weighted sampling and adaptive resampling. Studies have shown that when CARS is combined with PLS, it can significantly improve the predictive ability of the model. Specifically, the CARS-PLS model performed excellently in detecting the water core density and soluble solid content in apples, with R_p values and RMSEP values significantly lower than those of other models (Fig. 4a).[78] At the same time, Yao *et al.* pointed out that using a low-cost portable NIR spectrometer to detect the S-ovalbumin content in eggs, the model population analysis based on the Competitive Adaptive Reweighted Sampling (MPA-CARS) algorithm showed that its feature extraction performance was superior to that of CARS. The final simplified XGBoost model based on MPA-CARS feature wavelengths performed the best, with an R^2 of 0.906 and an RMSEP of 7.799%.[79] This indicated the effectiveness and applicability of patterns like CARS and PLS in infrared spectroscopy data analysis.

Meanwhile, the improved algorithms based on feature selection, such as the combination of Collaborative Interval PLS (Si-PLS) with CARS, have also been widely studied. When detecting myoglobin content in frozen pork, the Si-CARS-PLS

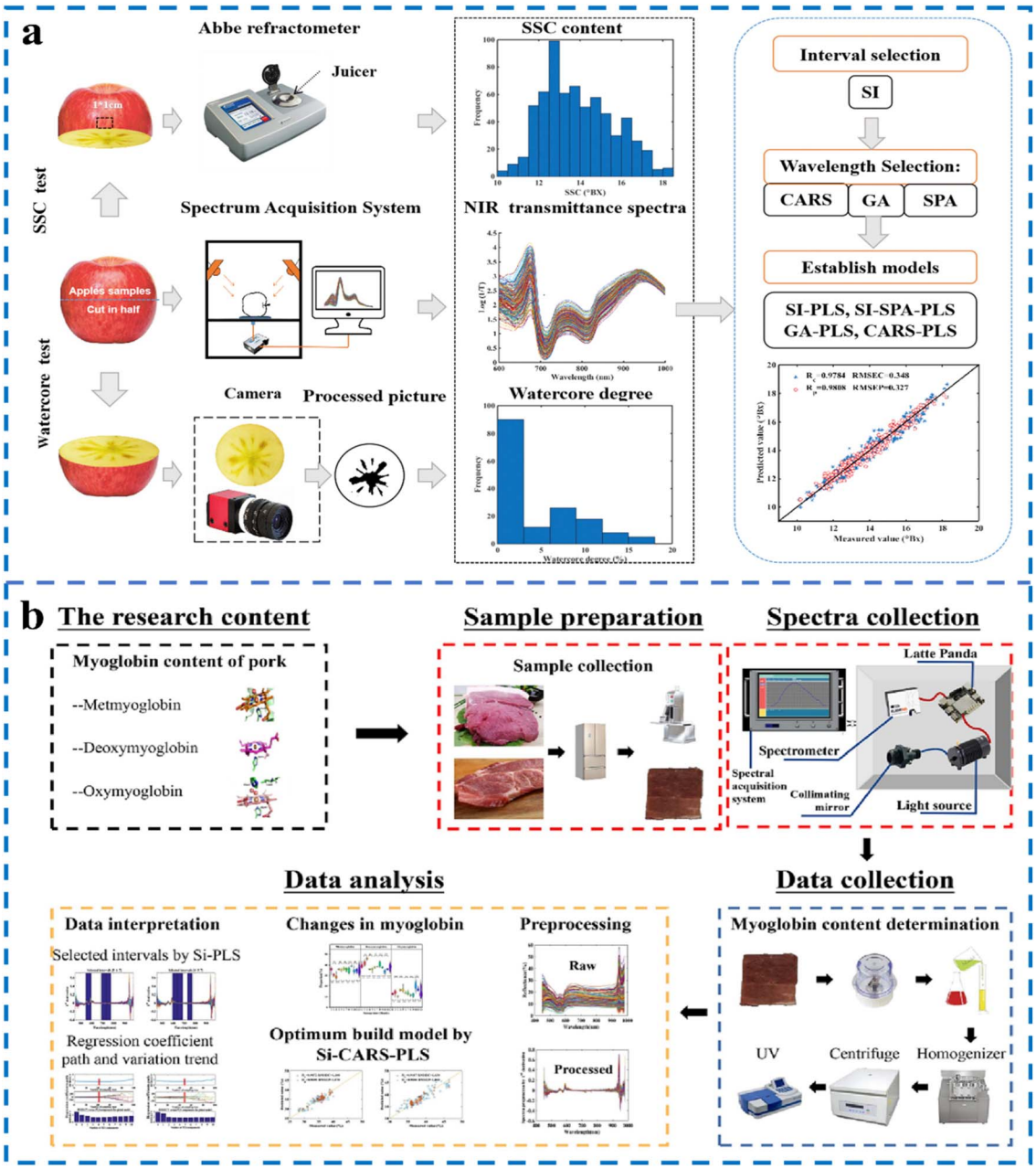

Fig. 4 (a) Flow chart of the experimental procedure to detect apple SSC and watercore degree by NIR system and using SI, GA, CARS, and SPA variable selection for building PLS models.[78] (b) Schematic illustration of detection of myoglobin content in pork meat during frozen storage using Vis-NIR spectroscopy.[80]

model showed R_p values above 0.8578, demonstrating its effectiveness and reliability in selecting important feature variables (Fig. 4b).[80] In addition, another study by Sun *et al.* used NIR-HSI to assess the viability of watermelon seeds. The SVM model achieved a 100% prediction accuracy, indicating that the HSI technology combined with the PCA-ABC-SVM model has practical application value in agricultural seed detection.[81] Therefore, feature variable selection not only improves the predictive accuracy but also effectively reduces the complexity of data processing, promoting the application of infrared spectroscopy in food safety testing.

4.2 Application of infrared spectroscopy technology in food safety and quality assessment

4.2.1. Agricultural product quality monitoring. Infrared spectroscopy technology has gained widespread attention in agricultural product quality monitoring, particularly in the detection of diseases and contaminants in major crops such as tea, corn, and wheat. Research has shown that infrared thermography technology can be effectively employed for detecting tea leaf diseases. Specifically, Yang *et al.* developed a fast method for detecting diseased areas in tea leaves using computer vision algorithms and infrared thermographic image

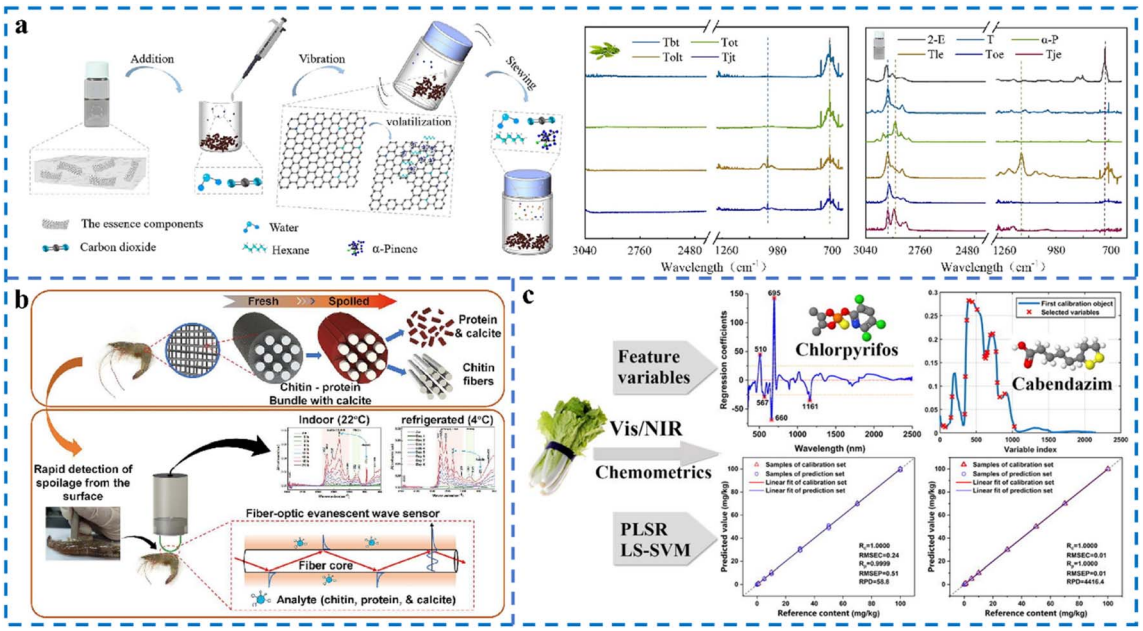

Fig. 5 Schematic diagram of infrared spectroscopy in different applications. (a) Detection of volatile organic compounds in adulterated tea using FTIR and PTR-MS.[83] (b) Non-destructive and *in situ* detection of shrimp freshness using mid-infrared fiber-optic evanescent wave spectroscopy.[90] (c) Detection of chlorpyrifos and carbendazim residues in the cabbage using Vis/NIR combined with chemometrics.[100]

processing techniques. The study found that the grayscale distribution of infrared images of tea leaf diseases has a certain regularity with the disease area. By extracting two feature parameters and applying them to a classifier, the assay accuracy was improved, with a correlation coefficient reaching 0.97, which is a 2% improvement over traditional algorithms.[82] In addition, Yang *et al.* utilized proton–transfer reaction mass spectrometry (PTR-MS) and FTIR to rapidly identify tea-adulterated liquid essences by detecting volatile organic compounds (VOCs). Results demonstrated prediction accuracies exceeding 0.941 for PTR-MS and 0.957 for FTIR, with LODs below practical application thresholds (Fig. 5a).[83]

In the case of corn, Wang *et al.* designed a NIR spectral acquisition device to assess protein content and insect infestation in maize seeds. In this study, SVM, logistic regression (LR), and partial least squares discriminant analysis (PLS-DA) were employed for the classification of insect-infested seeds, while PLS and least squares support vector machine (LS-SVM) were utilized for protein content detection. To reduce data redundancy and extract critical information, CARS and SPA were applied for feature wavelength selection. For the classification of insect-infested seeds, the CARS-SPA-LR model achieved an accuracy of 0.83 using only 7 feature wavelengths.[84] A study by Jiang *et al.* explored the combination of NIR and nano-modified colorimetric sensors for monitoring heavy metals (such as lead and mercury) in corn oil samples. The study showed that the developed sensor exhibited good accuracy in detecting heavy metals at low concentrations (10–100 ppb), with correlation coefficients of 0.9793 and 0.9510 for the prediction models, and LOD of 5 and 7 ppb, respectively.[85] Zheng *et al.* developed a method using NIR to detect Versicolorin A in corn. This method combined XGBoost with SVM to establish both a quantitative and a secondary classification approach. The root mean square error (RMSE) of the quantitative model prediction was 3.57 μg kg^{-1}, and the accuracy of the ranking method was 90.32%.[86]

In the case of wheat, Lin *et al.* proposed a novel method combining colorimetric sensors (CS) with VNIR to detect volatile markers in wheat infected by Aspergillus flavus. They established a Collaborative Interval Partial Least Squares (Si-PLS) model, with a correlation coefficient (R_p) of 0.9387 for the prediction model.[87] Zhao *et al.* combined CS with NIR to detect zearalenone (ZEN) in wheat and established a CNN model. The CNN model demonstrated superior predictive performance, with a coefficient of determination (R^2) of 0.91.[88] Almoujahed *et al.* used VNIR and mid-infrared spectroscopy (MIR) for non-destructive detection of Fusarium Head Blight (FHB) in wheat grains and flour.[89] These studies not only provide a fast and reliable method for agricultural product quality monitoring but also offer important references for research in related fields.

4.2.2. Food freshness evaluation. Infrared spectroscopy technology has also shown good application prospects in food freshness evaluation, especially in the monitoring of foods such as seafood and meat. Taking seafood as an example, Zhou *et al.* used mid-infrared fiber-optic evanescent wave (FOEW) spectroscopy to monitor the freshness of shrimp. By assessing the content of proteins, chitin, and calcite in the shrimp shells with the PLS-DA model, the researchers successfully achieved rapid, non-destructive detection of shrimp freshness. The results demonstrated that the PLS-DA model achieved recognition rates of 87.27% and 90.28% for the calibration and validation

sets, respectively (Fig. 5b).[90] Han *et al.* developed a non-destructive detection method for multiple freshness indicators (whiteness W, total volatile basic nitrogen TVB-N, and total viable count TVC) of crayfish during cold storage using NIRS integrated with deep learning. By comparing partial least squares regression (PLSR) and 1D convolutional neural network (1D-CNN) models, they found that the 1D-CNN model achieved optimal performance in predicting TVB-N and TVC, with R_p^2 values of 0.9397 and 0.9318 and RPD > 2.75, respectively, demonstrating superior accuracy in spectral analysis.[91] Zhou *et al.* developed a non-destructive and rapid detection method for freshness indicators (pH, TVB-N, TBARS, and K value) in bighead carp using NIRS combined with the CARS algorithm to optimize PLSR models. Based on 150 samples, the CARS-PLSR models achieved robust performance, with prediction correlation coefficients of 0.945 (pH), 0.932 (TVB-N), and 0.954 (TBARS), and RMSEP values below 0.107. These results validated the feasibility of NIRS technology for rapid freshness assessment in fish, providing a practical tool for quality monitoring in aquatic products.[92]

In the case of meat, Ouyang *et al.* developed a portable Vis-NIR spectroscopy system for rapid assessment of cooking loss rate in frozen pork, comparing the prediction performance of spectra from frozen and thawed states. Using the CARS-PLS model, they achieved prediction correlation coefficients of 0.8154 for frozen pork and 0.8421 for thawed pork, demonstrating comparable accuracy for both conditions.[93] Leng *et al.* established quantitative prediction models for TVB-N content in beef and pork using NIRS combined with PLS and SVR for the first time. The results showed that the PLS model based on raw spectra achieved optimal performance with a correlation coefficient of 0.9366 and a RMSEP of 3.15, while no spectral preprocessing methods improved model performance. In contrast, the SVR model exhibited weaker performance (R = 0.8314, RMSEP = 4.61). Variable Importance in Projection (VIP) analysis revealed that amino-containing compounds and lipids played critical roles in TVB-N prediction, highlighting their contribution to the PLS model's accuracy.[94] These studies demonstrate that infrared spectroscopy can effectively predict the freshness of food.

4.2.3. Detection of harmful substances in food. Infrared spectroscopy technology, due to its advantages of efficiency, speed, and non-destructiveness, has become one of the important detection methods for harmful substances in food. In the detection of mycotoxins, Caramês *et al.* explored the potential of NIR technology in detecting and classifying the content of Enniatins (ENNs) in barley grains. The study selected 60 barley samples from three different regions of Brazil, and the ENN content was determined using Ultra-Performance Liquid Chromatography-Tandem Mass Spectrometry (UPLC-MS/MS). Multivariate analysis models were constructed based on the NIR spectral data. The experimental results indicated a high

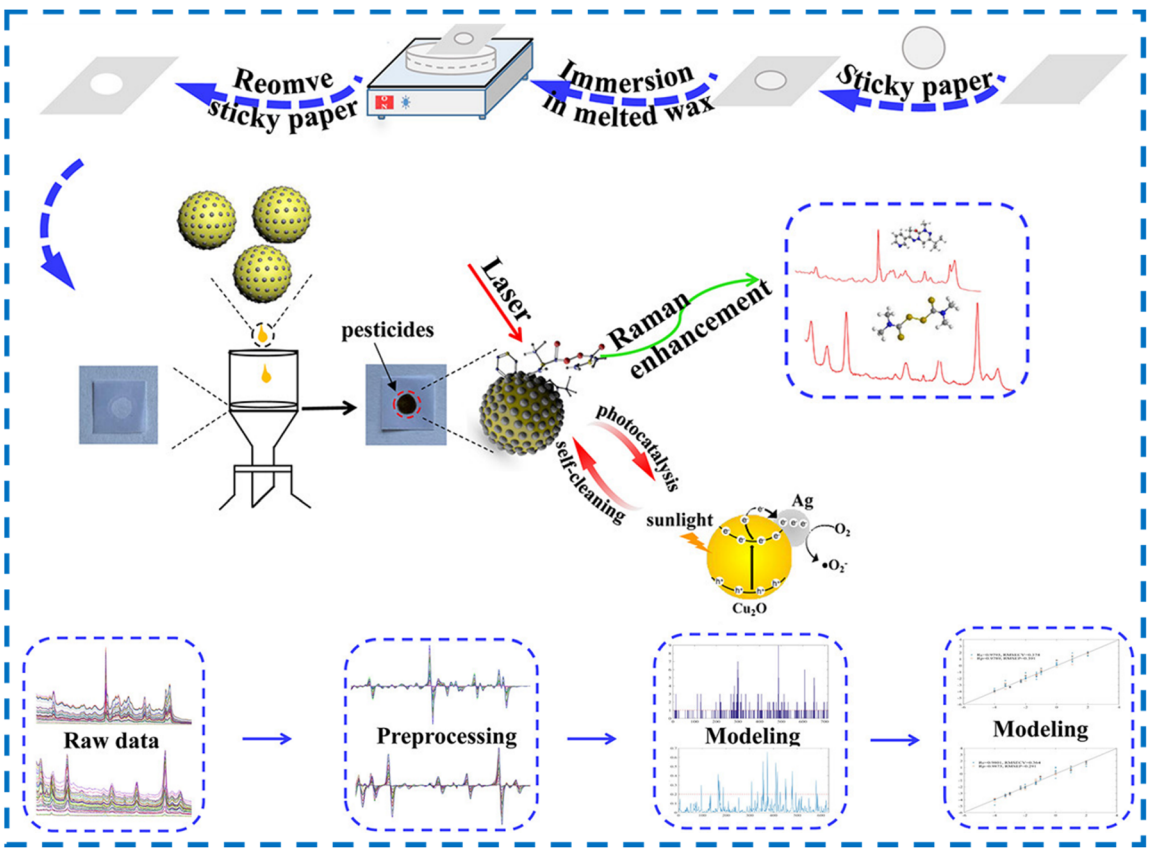

Fig. 6 Schematic illustration on MCu2O@Ag NPs-based SERS sensor and its detection and cleaning procedure of pesticides coupled with multivariate calibration.[104]

detection rate of ENNs in the barley samples (>70%). By processing the NIR data using PLS-DA models, the results demonstrated that the model performed well in distinguishing between contaminated and uncontaminated samples, with a sensitivity of 100% and a specificity of 94.2%.[95] Yao *et al.* developed a portable mid-infrared spectroscopy (FT-IR)-based non-destructive and rapid detection method for screening aflatoxin contamination in peanuts. By analyzing 274 peanut kernels inoculated with Aspergillus flavus strains and integrating chemometric models such as orthogonal partial least squares discriminant analysis(OPLS-DA), Soft independent modeling of class analogies (SIMCA), and PLSR, the method achieved high sensitivity (94.7%) in detecting samples with aflatoxin levels exceeding 3 ppb and demonstrated accurate quantification ($R_{pre} = 0.85$, RPD = 6.2).[96] These studies confirm that infrared spectroscopy technology, as a rapid and efficient detection method, holds significant potential for application in monitoring mycotoxin contamination.

In addition, in the field of heavy metal assay, Lin *et al.* explored a non-destructive detection method combining NIRS and chemoselective responsive dyes for the quantification of heavy metals Pb and Hg in edible oils. The olfactory visualization system was used to screen dyes, and synthesized porous silica nanospheres (PSNs) were employed to optimize the color sensor. The spectral data were preprocessed using SNV, and various chemometric models were applied to construct regression models. Among these, ant colony optimization- partial least squares (ACO-PLS) achieved optimal performance within the linear range of 0.001–100 ppm ($R_p^2 = 0.9612$), with a LOD of ≤1 ppb.[97] Miao *et al.* investigated the potential of NIRS combined with chemometric techniques for the quantitative analysis of Cd content in rice. By scanning 825 rice samples, the Kennard–Stone method was used to divide the samples into calibration and validation sets, and the spectra were preprocessed using the first derivative to reduce baseline drift. The study compared the performance of various chemometric algorithms (*e.g.*, iPLS, MWPLS, SiPLS, and biPLS) for extracting and optimizing spectral intervals, finding that the biPLS-based model performed the best, with a RMSEP of 0.2133, a correlation coefficient (R) of 0.9020, and a root mean square error of cross-validation (RMSECV) of 0.1756.[98] These studies prove that NIR is feasible for heavy metal detection in food.

At the same time, in the field of pesticide residue detection, Arzu Yazici *et al.* developed NIR combined with PLSR for rapid, non-destructive detection of boscalid and pyraclostrobin pesticide residues in strawberries, achieving predictive RPD values of 2.28 and 2.31, respectively.[99] Lu *et al.* used Vis/NIR combined with chemometrics to quantitatively analyze the residues of dichlorvos and carbendazim in cabbage. The quantitative models were developed using PLSR and LS-SVM models, with the LS-SVM model outperforming the PLSR model in determining pesticide residues in cabbage (Fig. 5c).[100] Rodriguez-Macadaeg *et al.* developed a LED-based near-infrared spectrometer for detecting pesticide residues of methyl parathion in rough rice, and white rice.[101] These studies indicate that infrared spectroscopy is an excellent technique for non-destructive detection of pesticide residues in fruits and vegetables.

5 SERS for food safety analysis

5.1 Basic principle of SERS

SERS is a highly sensitive spectroscopic technique that significantly enhances Raman signal intensity through the surface plasmon resonance (SPR) effect of metal nanostructures, enabling trace-level molecular detection.[102] The core principle of this technique lies in the localized electromagnetic field enhancement generated on the surface of metal nanostructures

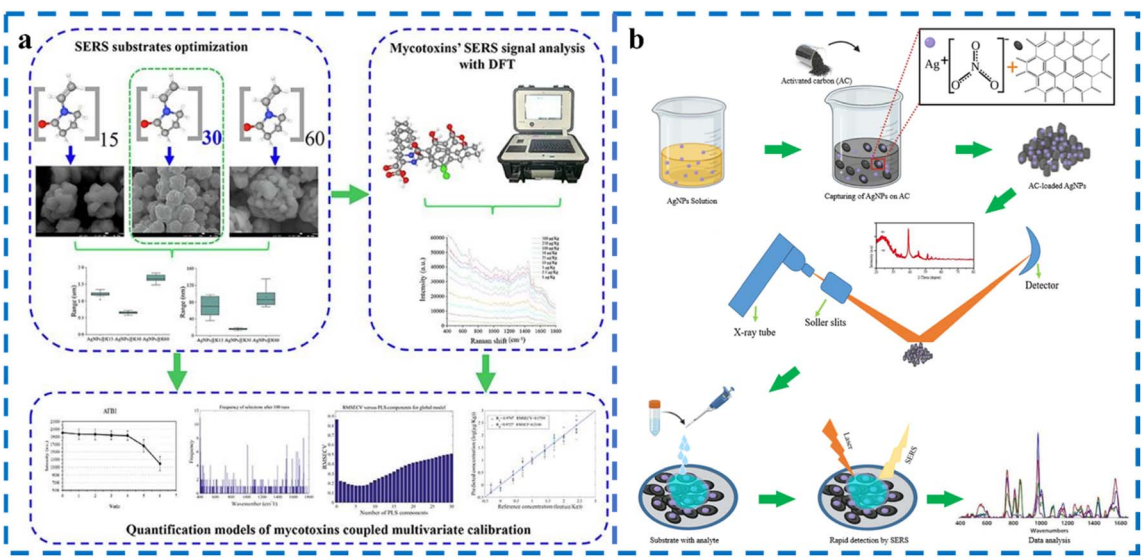

Fig. 7 Schematic diagram of SERS in different applications: (a) detection of three main mycotoxins in rice using SERS optimized AgNPs@K30 coupled multivariate calibration;[106] (b) activated carbon@silver nanoparticles conjugates as SERS substrate for capturing malathion analyte molecules for SERS detection[116]

(such as gold, silver, *etc.*), which can amplify Raman scattering signal intensity by 10^6 to 10^{14} times. The enhancement mechanisms of SERS are primarily divided into electromagnetic enhancement and chemical enhancement, with electromagnetic enhancement contributing approximately 10^4 to 10^{11} times, making it the dominant factor. Electromagnetic enhancement mainly relies on the SPR effect of metal nanostructures, while chemical enhancement involves charge transfer processes between molecules and the substrate.[103] For example, silver-coated Cu_2O mesoporous spheres (MCu_2O@Ag NPs) were used as a dual-function SERS chip, not only for the rapid detection of pymetrozine and thiram pesticides in tea samples but also for demonstrating photocatalytic activity in degrading pesticides under visible light (Fig. 6).[104]

5.2 Targeted detection of food hazards

5.2.1. Detection of toxins. SERS technology has demonstrated its superiority in the detection of toxins in food. For example, Guo *et al.* presents a label-free and highly sensitive detection approach for AFB1 utilizing SERS through a strategic design of aluminum ion-induced aggregation of iodine-modified silver nanoparticles, which generates localized electromagnetic hotspots. The developed method achieves a LOD as low as 0.47 fg mL^{-1}, surpassing the sensitivity thresholds of conventional detection techniques.[105] Similarly, in the monitoring of multiple mycotoxins, a sensor using functionalized AgNPs as SERS probes demonstrated excellent sensitivity and accuracy, especially in monitoring AFB1, OTA, and OTB in rice samples. The LOD were 1.145, 1.133, and 1.180 μg Kg^{-1}, respectively, with good stability and repeatability (Fig. 7a).[106] Chen *et al.* used Au@SiO_2 substrates to establish a SERS-based lateral flow immunoassay for the simultaneous detection of AFB1 and OTA. Through systematic optimization of experimental conditions, the biosensor demonstrated high sensitivity and reusability, with LOD of 0.24 pg mL^{-1} for AFB1 and 0.37 pg mL^{-1} for OTA, which are far below the LOD set by the European Commission.[107] Xu *et al.* prepared a gold–silver bilayer@gold nanoparticle (Au–Ag Janus@Au NPs) SERS-active substrate by regulating pH. This substrate has tunable hollow nanostructures and enables sensitive and reliable assay of trace amounts of staphylococcal enterotoxins in food, with a LOD as low as 0.55 pg mL^{-1}.[108]

In recent years, SERS technology for detecting ZEN have emerged as a research hotspot, driven by their advantages in sensitivity, rapidity, and non-destructiveness. Guo *et al.* developed a SERS aptasensor by fabricating mesoporous silica-supported gold nanocomposites (MSN-Rh6G-AuNPs) as the SERS substrate, followed by aptamer functionalization, enabling highly sensitive and quantitative detection of ZEN with a LOD as low as 0.0064 ng mL^{-1}.[109] Yin *et al.* developed a SERS-based test strip utilizing core–shell Au@Ag nanoparticles (Au@AgNPs) embedded with reporter molecules (4-MBA) as SERS nanoprobes, achieving highly sensitive detection of ZEN in corn with a detection range of 10–1000 μg kg^{-1} and a LOD as low as 3.6 μg kg^{-1}.[110] Zhu *et al.* employed SERS combined with a deep learning model to detect ZEN in corn oil, with a LOD of 6.81×10^{-4} μg mL^{-1}, demonstrating the potential of SERS for application in complex matrices.[111]

Additionally, Xue *et al.* developed a SERS aptasensor based on a two-dimensional film-like structure, utilizing GO@Au nanosheets as capture probes and core–shell Au@Ag nanoparticles as signal probes. Through a competitive binding mechanism, the sensor achieved highly sensitive detection of patulin (PAT) in apples, with a detection range of 1–70 ng mL^{-1} and a LOD as low as 0.46 ng mL^{-1}.[112] Guo *et al.* integrated SERS with the coffee-ring effect to achieve high-throughput, label-free detection of PAT and alternariol (AOH) in fruits and their products. By optimizing drying temperature and droplet volume, a stable coffee-ring structure was constructed, and synergy interval (Si) and genetic algorithm (GA) were employed for variable selection. The method demonstrated a LOD as low as 1 μg L^{-1}, showcasing its potential for rapid and sensitive mycotoxin analysis in complex food matrices.[113] Li *et al.* developed a flexible paper-based SERS sensor utilizing flower-like AgNPs combined with artificial intelligence tools, achieving picogram-level highly sensitive detection of chloramphenicol (CAP) in food samples. The method demonstrated a detection range of 10^2–10^{-5} μg mL^{-1} and a LOD as low as 10^{-5} μg mL^{-1}.[114] Wu *et al.* developed a highly sensitive competitive SERS sensor based on aptamer-modified Au@Ag nanoparticles and gold nanostars (AuNSs) plasmonic nanocomposites, achieving rapid detection of PAT in apples and their products with a LOD as low as 0.0281 ng mL^{-1}.[115] These studies suggest that SERS technology shows great promise for the rapid detection of toxins in food. It not only offers high sensitivity and accuracy but also adapts well to complex food matrices, providing strong support for food safety.

5.2.2. Detection of pesticide residues. Studies have shown that, malathion, a commonly used organophosphate pesticide, can cause damage to the nervous system of humans and animals when exposed to high concentrations. Aheto *et al.* developed a carbon-based colloidal surface-enhanced SERS active substrate, demonstrating good quantitative analysis capabilities of malathion (Fig. 7b).[116] In addition, another study used silver nanoflowers as a SERS substrate to successfully detect residues of chlorpyrifos and carbamate pesticides in rice. The results showed a significant linear relationship and low LOD, indicating that this method is suitable for food safety monitoring.[117] At the same time, Ma *et al.* also demonstrated a SERS immunosensor based on carbamates and thiamethoxam, which can achieve highly sensitive assay of pesticides in complex environments. The LOD reached 1.22 μM and 0.076 μM, indicating the potential application of this sensor in food safety testing.[118] Bai *et al.* loaded AgNPs onto water-based polyurethane (WPU) to prepare a high-viscosity WPU@AgNPs substrate tape for detecting thiabendazole residues on the surfaces of pears, apples, and bananas. The LOD were 1.44, 1.12, and 1.63 ng cm^{-2}, respectively, making it a commonly used pattern for rapid, ultra-sensitive detection of thiabendazole residues in the field.[119] Pan *et al.* developed a SERS method combining gold nanorods and chemometrics for the rapid quantitative assay of thiabendazole (TBZ) in citrus, achieving an accuracy of up to 99.17%.[120]

In addition, researchers have also explored the application of other SERS substrates. For example, Sun *et al.* developed a composite substrate modified with three-dimensional gold

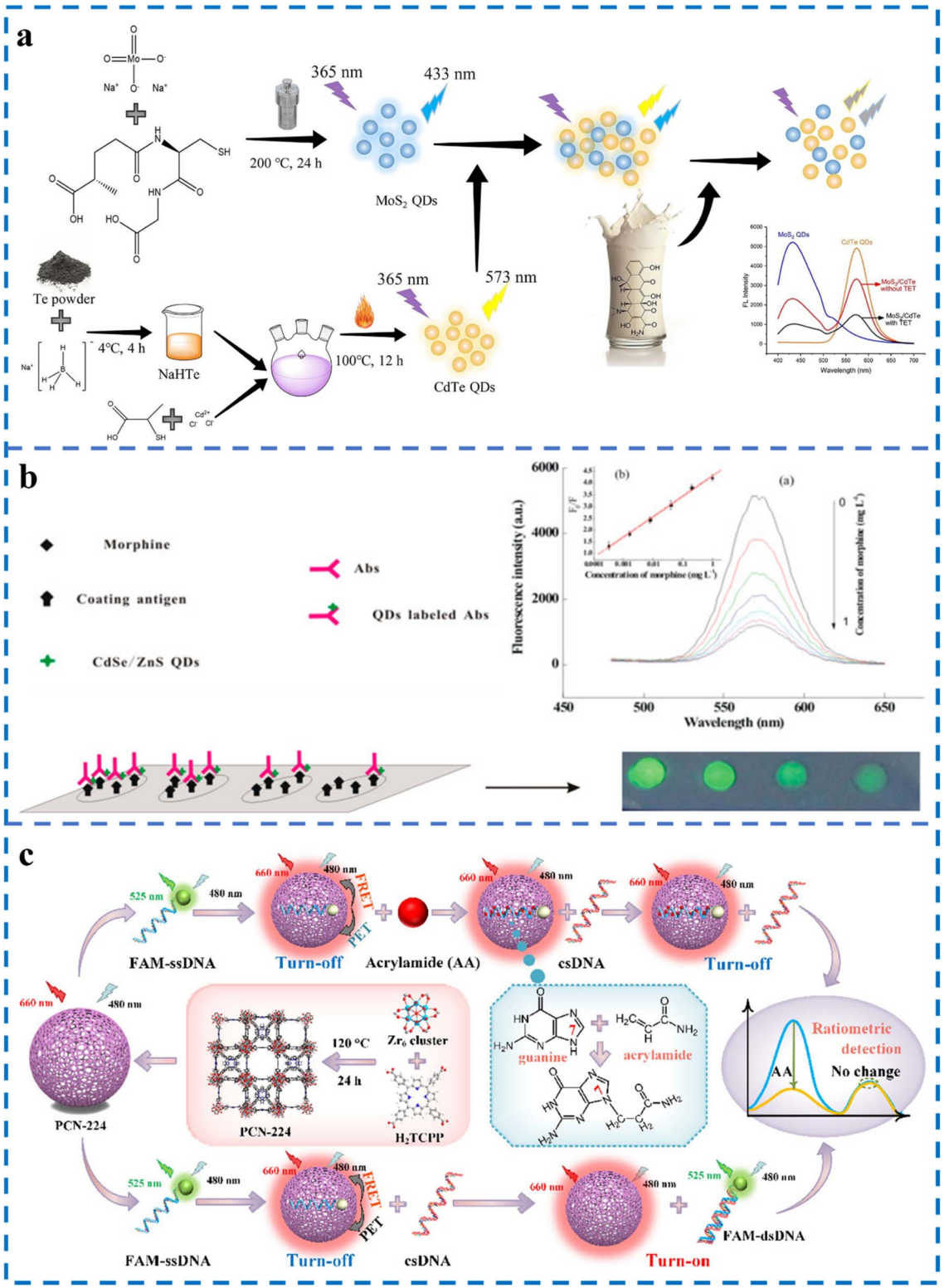

Fig. 8 Principle and construction of fluorescent sensors: (a) principle diagram for TET detection based on MoS_2 QDs and CdTe QDs;[125] (b) the QDs labeled antimorphine antibodies (QDs labeled Abs) fluorescence immunoassays;[126] (c) illustration of the determination process of the PCN-224 biosensor for rapid and sensitive detection of acrylamide.[133]

nanodendrites (AuNDs) and AgNPs, which can sensitively detect melamine and thiamethoxam in food samples, with LOD of 7.38 μg L^{-1} and 86.1 μg L^{-1}, respectively.[121] In a study by Wei *et al.*, a method combining a polymer substrate with gold–silver nanocomposites was successfully used for the non-destructive assay of carbendazim on apple skins,

verifying excellent sensitivity and selectivity.[122] Huang *et al.* used a three-dimensional SERS substrate composed of AgNPs, and polyacrylonitrile successfully detected carbendazim residues in apple samples, showing good recovery and relative standard deviation.[123] These studies indicate that SERS technology has broad application prospects in pesticide residue detection, providing a rapid and sensitive means of ensuring food safety.

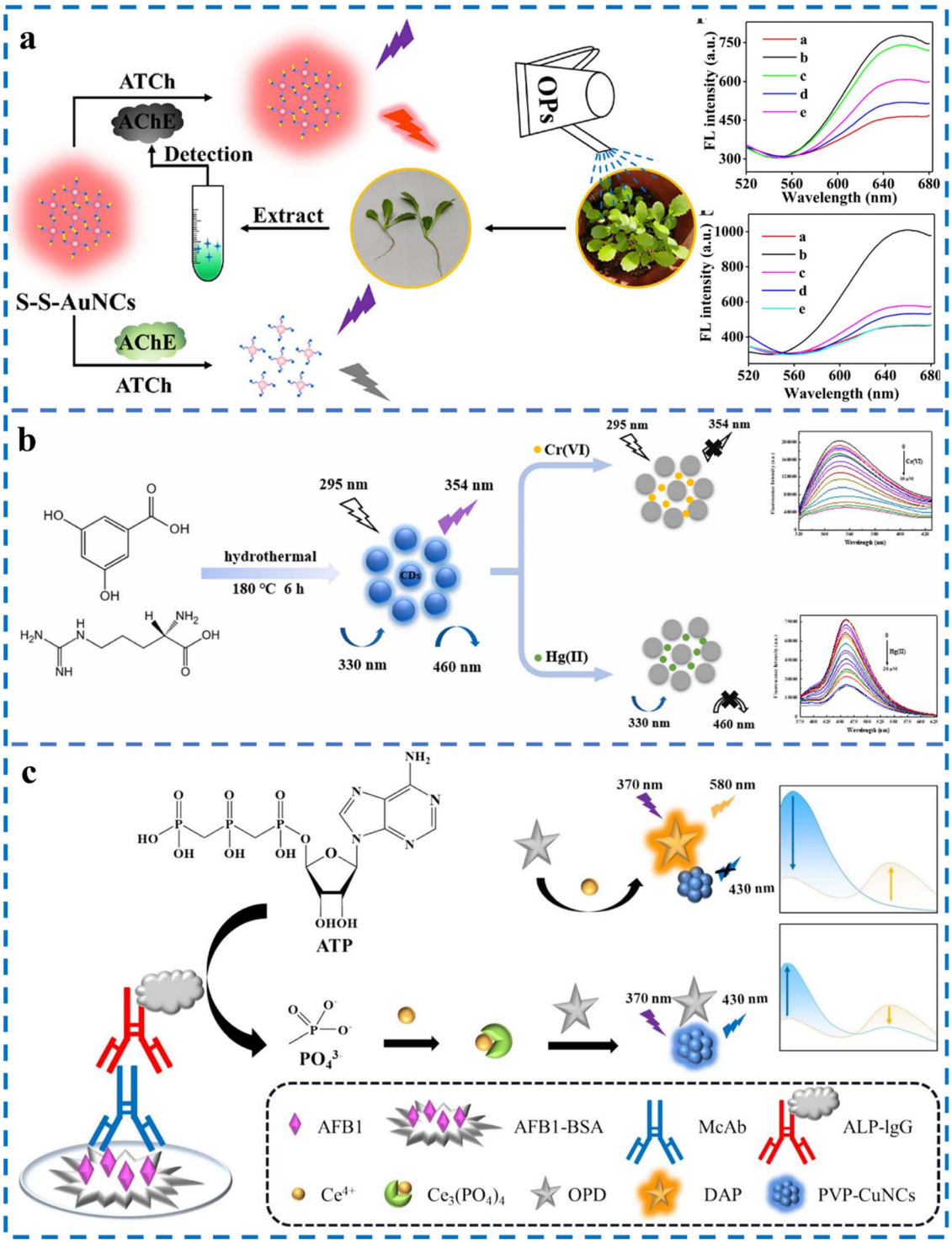

Fig. 9 Schematic diagram of fluorescence sensing technology in different applications. (a) pH and redox dual-response disulfide bond-functionalized red-emitting gold nanoclusters for monitoring the contamination of organophosphorus pesticides in foods.[135] (b) A fluorescent probe based on carbon quantum dots with spectral selectivity for sensitive detection of Cr(VI) and Hg(II).[141] (c) A ratiometric fluorescence immunoassay based on Ce^{4+} oxidized *o*-phthalylenediamine and polyvinylpyrrolidone protected copper nanoclusters for the detection of aflatoxin B1.[145]

6 Fluorescence sensing for food safety analysis

6.1 Principle and construction of fluorescence sensors

Fluorescence sensing technology utilizes the specific binding between receptors and target analytes, leading to changes in fluorescence signals such as enhanced or quenched fluorescence intensity, blue shift or red shift of wavelength, *etc.*, to achieve detection of the target substance.[124] There are various methods for constructing fluorescence sensors, which primarily depend on the selection of fluorescent materials and the design of the sensing mechanism. In recent years, QDs have become popular materials in fluorescence sensor research. For example, Liang *et al.* developed a dual-signal fluorescent sensor based on molybdenum disulfide quantum dots (MoS_2 QDs, blue emission at 433 nm) and cadmium telluride quantum dots (CdTe QDs, yellow emission at 573 nm) for highly sensitive detection of tetracycline (TET) in milk samples (Fig. 8a).[125] Zhang *et al.* developed a fluorescence immunoassay (FLISA) based on quantum dot (CdSe/ZnS)-labeled antibodies for highly sensitive detection of morphine (Fig. 8b).[126]

Fluorescent signal modulation mechanisms primarily include "turn-on," "turn-off," and ratiometric sensing. The "turn-on" mechanism refers to the enhancement of fluorescence intensity upon the specific binding of the sensor to the target analyte.[127] This mechanism typically relies on the suppression of static or dynamic quenching effects, such as fluorescence resonance energy transfer (FRET), inner filter effect (IFE), or photoinduced electron transfer (PET). A particularly promising subclass of "turn-on" sensing is based on the aggregation-induced emission (AIE) phenomenon, wherein fluorophores exhibit weak or no emission in the molecularly dispersed state but emit strongly upon aggregation. AIE-based sensors overcome the limitations of traditional fluorophores affected by aggregation-caused quenching (ACQ), offering enhanced photostability, strong signal intensity in aqueous or complex food matrices, and low background interference. Its advantage lies in the amplified signal, which effectively minimizes background interference and improves detection sensitivity. However, the presence of other fluorescent substances in the environment may also cause non-specific enhancement, potentially compromising specificity and reliability.[128]

In contrast, the "turn-off" mechanism is based on fluorescence quenching, where the fluorescence signal significantly decreases upon target recognition.[129] This mechanism often utilizes static or dynamic quenching principles, such as π–π interactions between quenchers and fluorophores or energy absorption by heavy metal ions. Its strength lies in its applicability in high-background fluorescence environments and, in some cases, its broad linear detection range. However, the decrease in fluorescence intensity may be influenced by environmental factors, such as photobleaching or background fluorescence fluctuations, leading to potential misinterpretation or reduced sensitivity.[130]

To address the limitations of single-signal fluorescence modes, ratiometric sensing has gained significant attention. Ratiometric sensing typically relies on the relative intensity changes of two fluorescence channels, where the presence of the target analyte induces a quantifiable ratio change rather than mere enhancement or attenuation of a single channel.[131] Common ratiometric designs include FRET-based probes, dual-emission fluorophore-labeled probes, and environmentally responsive fluorescent nanomaterials. Its advantages include effective reduction of background fluorescence interference, improved accuracy and reproducibility, and a broader dynamic detection range.[132] For example, Gan *et al.* developed a ratio fluorescence biosensor based on 6-carboxyfluorescein-labeled aptamers (FAM-ssDNA) and the metal–organic framework (PCN-224), which can detect the neurotoxin and carcinogen acrylamide formed in food. The detection range is from 10 nM to 0.5 mM, with a LOD of 1.9 nM, demonstrating its potential application in thermally processed foods (Fig. 8c).[133]

6.2 Targeted detection of food hazards

6.2.1. Detection of pesticide residues. In recent years, the application of fluorescence sensors in the field of food safety has received widespread attention, especially with significant progress in the detection of pesticide residues. Research has shown that fluorescence-based sensors can achieve high sensitivity and selectivity for detecting various pesticides. For example, Qiu *et al.* developed a fluorescence sensor based on MIPs for detecting residues of the pesticide bifenthrin (BC). The sensor uses SiO_2 as a carrier and synthesizes FMIPs through precipitation polymerization, showing a good linear relationship within the concentration range of 10.11–80 nM, with a correlation coefficient of 0.9919 and a LOD of 10.11 nM. This research demonstrates the promising potential of FMIPs in the detection of agricultural products.[134] Li *et al.* developed a high-performance fluorescence sensor for detecting organophosphorus pesticides (OPs) based on hydrolysis-responsive disulfide bond-functionalized gold nanoclusters (S–S–AuNCs) (Fig. 9a).[135] Zhang *et al.* focused on the development of a fluorescence sensor for carbaryl. The researchers used a combination of QDs and MIPs, modifying the surface of QDs through electrostatic interactions to construct a QDs@MIP sensor. During detection, the sensor exhibited selective recognition of carbaryl and showed good correlation with the results of high-performance liquid chromatography (HPLC) and enzyme-linked immunosorbent assay (ELISA) methods ($R^2 = 0.98$), demonstrating its potential application in food safety detection.[136] Ouyang *et al.* developed a highly sensitive biosensor for carbendazim (CBZ) detection based on luminescent resonance energy transfer (LRET) between upconversion nanoparticles (UCNPs, donor) and manganese dioxide (MnO_2, acceptor) nanosheets. In the presence of CBZ, its specific binding to the aptamer triggered the detachment of UCNPs-aptamer from MnO_2 nanosheets, resulting in fluorescence recovery. The sensor exhibited a linear response over the range of 0.1–5000 ng mL^{-1}, with a LOD as low as 0.05 ng mL^{-1}.[137]

In addition, Wang *et al.* developed a multiplex biosensor based on FRET that can simultaneously and selectively detect multiple pesticides in food, such as paraquat and carbendazim. The sensor exhibited good linear correlation and low LOD of 0.18 ng mL^{-1}

and 0.45 ng mL^{-1}, respectively.[138] These research findings indicate that fluorescence sensors offer high sensitivity, strong selectivity, and ease of operation in pesticide residue detection, providing effective technical support for food safety monitoring. While fluorescence-based sensors have demonstrated high sensitivity for detecting trace levels of pesticide residues, their real-world applicability still faces limitations. Fluorescence quenching caused by pigments, polyphenols, or other matrix constituents in fruits and vegetables can severely affect signal stability. Moreover, most current systems rely on ideal lab conditions, and their performance may vary significantly under field conditions due to fluctuations in temperature, humidity, and light. Additionally, non-specific binding in antibody- or aptamer-based sensors may lead to cross-reactivity with structurally similar compounds, increasing the risk of false positives. To ensure reliable detection, further improvements in selectivity, robustness, and miniaturization are necessary for effective on-site pesticide screening.

6.2.2. Detection of heavy metals. In recent years, fluorescence-based methods for detecting heavy metal ions have garnered increasing attention, especially in the field of food safety monitoring. For example, a novel ratio fluorescence probe has been proposed for detecting Pb^{2+} in food, based on the combination of copper nanoclusters (CuNCs) and nitrogen-doped carbon quantum dots (CNQDs). In this probe, CuNCs provide the response signal, with fluorescence enhanced due to the aggregation-induced emission enhancement (AIEE) effect in the presence of Pb^{2+}. Additionally, CNQDs offer a self-calibrating signal, with fluorescence remaining almost unchanged in the presence of Pb^{2+}. By monitoring the change in the fluorescence intensity ratio, sensitive detection of Pb^{2+} can be achieved, with a detection range of 0.010–2.5 mg L^{-1} and a LOD of 0.0031 mg L^{-1}. This study demonstrates a simple, stable, and sensitive method for detecting Pb^{2+}.[139] Hassibian *et al.* developed a sensitive fluorescence aptamer sensor for detecting Pb^{2+} by using hollow gold nanoparticles (HGNPs) as the nanocarrier and rhodamine B (RDB) fluorescence dye as the signaling agent.[140] Fluorescent carbon QDs were synthesized using a hydrothermal method with 3,5-dihydroxybenzoic acid and L-arginine. The prepared fluorescence sensor can detect Hg^{2+} in tap water and lake water, with a LOD of 0.084 μm (Fig. 9b).[141] In addition, Li *et al.* designed a microfluidic fluorescence sensor array by combining microfluidic sensing and organic fluorescence switches, which enables real-time and synchronous visual assay of multiple-component heavy metal ions.[142]

Wang *et al.* developed a dual-signal fluorescent sensor based on the cascade catalytic reactions of acetylcholinesterase (AChE) and choline oxidase (ChOx) for highly sensitive detection of OPs. This method exhibited a linear detection range of 10–2000 ng mL^{-1} with a detection limit as low as 2.05 ng mL^{-1}. By integrating smartphone-based color recognition and a WeChat mini-program, it enabled rapid on-site analysis of OPs residues, demonstrating significant potential for practical applications in food safety monitoring.[143] These applications of fluorescence sensors in food safety evaluation further confirm their effectiveness and potential in heavy metal monitoring. Despite the excellent sensitivity of fluorescence sensing in detecting metal ions like Hg^{2+}, Pb^{2+}, or Cd^{2+}, selectivity remains a major challenge. Many fluorescence probes suffer from interference by co-existing metal ions with similar binding affinities, especially in complex matrices such as tea, grains, or seafood. Furthermore, the dependence on precise pH or ionic strength for optimal probe performance limits the robustness of detection in variable environments. Fluorescent nanomaterials, though promising, may also pose toxicity concerns if not properly immobilized or purified, restricting their practical use in food-contact applications. Therefore, developing highly selective, environmentally stable, and biocompatible fluorescence platforms is essential for future progress.

6.2.3. Detection of mycotoxins. As secondary metabolites of fungi, mycotoxins affect one-quarter of the world's food crops every year, leading to food losses. Therefore, the development of fluorescence sensing technologies for detecting mycotoxins is essential. Dou *et al.* developed a ratio fluorescence method based on a nanometal–organic framework aptamer sensor to detect AFB1. The results showed high sensitivity and specificity, with a linear range of 0–3.33 ng mL^{-1} and a LOD of 0.08 ng mL^{-1}.[144] Sun *et al.* established a ratio fluorescence method for detecting AFB1 based on Ce^{4+} oxidation of *o*-phenylenediamine (OPD) and polyethyleneimine-protected copper nanoclusters (PVP-CuNC). The results showed that this method had a LOD of 26.79 pg mL^{-1} and a linear detection range of 50–250 pg mL^{-1} (Fig. 9c).[145] Bi *et al.* developed a ratio fluorescence sensor based on nitrogen-doped graphene quantum dots (NGQDs-apt) and silica-encapsulated cadmium telluride quantum dots (CdTe QDs @ SiO_2), which enables accurate analysis of ZEN in corn and barley flour. The sensor demonstrated excellent performance with a LOD of 0.32 pg mL^{-1}.[146] In another study, a capillary-based immunofluorescence sensor was developed to detect ZON, with a LOD of 0.003 ng mL^{-1} and a quantification limit (LOQ) of 0.007 ng mL^{-1}.[147] These findings demonstrate that fluorescence sensors provide effective technical support in the detection of mycotoxins. The application of fluorescence sensors in detecting mycotoxins—such as aflatoxins or ochratoxins—has yielded promising LODs; however, several obstacles remain. Most notably, complex food matrices such as grains, nuts, and fermented products often contain natural fluorescent compounds that interfere with signal readout, complicating quantitative analysis. Additionally, achieving multiplex detection of co-existing mycotoxins remains technically challenging due to overlapping emission spectra. Sensor stability over time and during storage is also a concern, especially for field-deployable kits. To overcome these limitations, future strategies should focus on ratiometric detection, AIE-based materials, and integrated microfluidic fluorescence systems that enhance anti-interference capabilities and standardization.

7 Summary and outlook

Non-destructive analytical technologies have revolutionized food safety and quality assessment, yet their distinct operational principles, performance metrics, and application scopes necessitate a systematic comparative analysis to guide technology selection. HSI excels in spatially resolved chemical

mapping due to its unique fusion of spectral and spatial data. However, its reliance on high-resolution cameras and spectral preprocessing algorithms limits real-time deployment, while its detection sensitivity is inferior to electrochemical sensing, which achieves attomolar-level LODs through nanomaterial-enhanced signal amplification. Electrochemical platforms, such as Ti_3C_2-based sensors for DON, prioritize portability and rapid response but struggle with multiplex detection in complex matrices due to cross-reactive interference. In contrast, infrared spectroscopy (NIR/FTIR) offers reagent-free, high-throughput screening for bulk composition analysis but lacks molecular specificity compared to SERS. SERS leverages plasmonic nanostructures for single-molecule sensitivity and fingerprint specificity, yet its performance is highly substrate-dependent, requiring meticulous optimization to mitigate food matrix effects. Fluorescence sensing, particularly ratiometric designs, balances sensitivity and anti-interference capability through dual-channel signal modulation but faces challenges in photostability and field adaptability due to ambient light interference.

Current limitations stem from several critical gaps: (1) reliance on laboratory-grade instrumentation and skilled operators impedes real-time field deployment; (2) signal attenuation or misinterpretation persists in heterogeneous, high-fat, or high-moisture matrices; (3) algorithm generalizability and cross-platform validation frameworks are underdeveloped; (4) integrated multimodal systems and data fusion strategies lack maturity. Future efforts should prioritize: (1) miniaturized, cost-effective devices coupled with edge computing and IoT for decentralized monitoring; (2) AI-driven advancements to enhance feature extraction and model adaptability across diverse food categories (3) synergistic multimodal approaches (*e.g.*, HSI-SERS hybridization, electrochemical-fluorescence coupling); to overcome single-technology constraints, augmented by blockchain-enabled traceability for supply chain transparency; (4) innovative functional materials to improve sensor selectivity, stability, and environmental resilience.

Looking ahead, the evolution of non-destructive technologies promises transformative impacts on food safety governance. Breakthroughs in smart algorithms, nanomaterial engineering, and interdisciplinary integration will drive next-generation systems toward higher precision, lower costs, and full automation. Such advancements will not only enable early risk and targeted interventions but also foster resource-efficient detection paradigms, supporting the green transition and resilience of global food systems. Through collaborative efforts among academia, industry, and policymakers, non-destructive technologies are poised to become cornerstones of food safety infrastructure, safeguarding public health and advancing sustainable development goals with robust technical assurance.

Data availability

No primary research results, software or code have been included and no new data were generated or analysed as part of this review.

Author contributions

Yuerong Feng: writing – original draft; Xinai Zhang: review and editing; Jiaqian Liu: reviewing; Zhecong Yuan: reviewing; Shujie Gao: reviewing; Jiyong Shi: review and editing.

Conflicts of interest

The authors declare no conflict of interest.

References

1 P. Zhang, J. Su, H. Zhen, T. Yu, L. Wei, M. Zheng, C. Zeng and W. Shu, *Coord. Chem. Rev.*, 2025, **522**, 216232.
2 C. Tang, Y. He, B. Yuan, L. Li, L. Luo and T. You, *Compr. Rev. Food Sci. Food Saf.*, 2024, **23**, e70062.
3 S. Y.-S. S. Adade, H. Lin, N. A. N. Johnson, X. Nunekpeku, J. H. Aheto, J.-N. Ekumah, B. A. Kwadzokpui, E. Teye, W. Ahmad and Q. Chen, *Trends Food Sci. Technol.*, 2025, **156**, 104851.
4 X. Zhang, X. Huang, Z. Wang, Y. Zhang, X. Huang, Z. Li, M. Daglia, J. Xiao, J. Shi and X. Zou, *Chem. Eng. J.*, 2022, **429**, 132243.
5 L. Shi, Y. Li, C. Jia, J. Shan, S. Wang, S. Liu, J. Sun, D. Zhang, Y. Ji and J. Wang, *Trends Food Sci. Technol.*, 2023, **138**, 100–115.
6 X. Zhang, Z. Wang, X. Huang, Q. Huang, Y. Wen, B. Li, M. Holmes, J. Shi and X. Zou, *Chem. Eng. J.*, 2023, **451**, 138928.
7 M. Angelopoulou, P. Petrou and S. Kakabakos, *Trac. Trends Anal. Chem.*, 2024, **175**, 117714.
8 Y. Li, W. Zhang, Z. Cui, L. Shi, Y. Shang, Y. Ji and J. Wang, *Trends Food Sci. Technol.*, 2024, **149**, 104564.
9 L. Liu, Y. Wang, Z. Xue, B. Peng, X. Kou and Z. Gao, *Trends Food Sci. Technol.*, 2024, **148**, 104487.
10 H. Pu, T. Fang, Z. Wu and D.-W. Sun, *Trends Food Sci. Technol.*, 2023, **138**, 697–707.
11 X. Zhang, Y. Zhou, X. Huang, X. Hu, X. Huang, L. Yin, Q. Huang, Y. Wen, B. Li, J. Shi and X. Zou, *Food Chem.*, 2023, **407**, 135115.
12 Y. Pu, Y. Feng and D. Sun, *Compr. Rev. Food Sci. Food Saf.*, 2015, **14**, 176–188.
13 W.-H. Chen, S. Maheshwaran, Y.-K. Park and H. C. Ong, *Sci. Total Environ.*, 2024, **953**, 176128.
14 W. Qi, Y. Tian, D. Lu and B. Chen, *Foods*, 2022, **11**, 930.
15 N. Logan, C. Cao, S. Freitag, S. A. Haughey, R. Krska and C. T. Elliott, *Adv. Mater.*, 2024, **36**, 2309625.
16 T. Du, L. Huang, J. Wang, J. Sun, W. Zhang and J. Wang, *Trends Food Sci. Technol.*, 2021, **111**, 716–730.
17 G. Jaiswal, R. Rani, H. Mangotra and A. Sharma, *Comput. Sci. Rev.*, 2023, **50**, 100584.
18 H. Pu, Q. Wei and D.-W. Sun, *Crit. Rev. Food Sci. Nutr.*, 2023, **63**, 1297–1313.
19 H.-J. He and D.-W. Sun, *Trends Food Sci. Technol.*, 2015, **46**, 99–109.

20 S. S. Tunny, H. Kurniawan, H. Z. Amanah, I. Baek, M. S. Kim, D. Chan, M. A. Faqeerzada, C. Wakholi and B.-K. Cho, *Postharvest Biol. Technol.*, 2023, **201**, 112373.
21 Z. Zhou, Y. Zhang, Y. Xie, T. Huang, Z. Li, P. Chen, Y. Lu, S. Yu, S. Zhang and G. Zheng, *Light Sci. Appl.*, 2024, **13**, 242.
22 M. Xu, J. Sun, K. Yao, X. Wu, J. Shen, Y. Cao and X. Zhou, *J. Food Sci.*, 2022, **87**, 326–338.
23 H. Li, Q. Chen, J. Zhao and M. Wu, *LWT–Food Sci. Technol.*, 2015, **63**, 268–274.
24 J. Sun, J. Cheng, M. Xu and K. Yao, *J. Food Compos. Anal.*, 2024, **129**, 106144.
25 K. Yao, J. Sun, C. Chen, M. Xu, X. Zhou, Y. Cao and Y. Tian, *J. Food Eng.*, 2022, **325**, 111024.
26 K. Yao, J. Sun, X. Zhou, A. Nirere, Y. Tian and X. Wu, *J. Food Process Eng.*, 2020, **43**, e13422.
27 K. Yao, J. Sun, L. Zhang, X. Zhou, Y. Tian, N. Tang and X. Wu, *J. Food Saf.*, 2021, **41**, e12888.
28 X. Tang, L. Rao, L. Xie, M. Yan, Z. Chen, S. Liu, L. Chen, S. Xiao, N. Ding, Z. Zhang and L. Huang, *Meat Sci.*, 2023, **196**, 109052.
29 J. Cheng, J. Sun, M. Xu and X. Zhou, *J. Food Compos. Anal.*, 2023, **123**, 105497.
30 C. Dong, Y. Ye, J. Zhang, H. Zhu and F. Liu, *J. Integr. Agric.*, 2014, **13**, 2229–2235.
31 J. Zhao, H. Li, C. Chen, Y. Pang and X. Zhu, *Agriculture*, 2022, **12**, 1796.
32 Y. Hu, H. Yu, X. Song, W. Chen, L. Ding, J. Chen, Z. Liu, Y. Guo, D. Xu, X. Zhu, C. Zhou, J. Zhang, B. Liao, J. Zhou, X. Li, Y. Wang and Y. He, *Food Res. Int.*, 2024, **196**, 115110.
33 A. Nirere, J. Sun, R. Kama, V. A. Atindana, F. D. Nikubwimana, K. D. Dusabe and Y. Zhong, *J. Food Process Eng.*, 2023, **46**, e14293.
34 J. Sun, S. Cong, H. Mao, X. Wu and N. Yang, *J. Food Process Eng.*, 2018, **41**, e12654.
35 T. Xiao, L. Yang, X. He, L. Wang, D. Zhang, T. Cui, K. Zhang, L. Bao, S. An and X. Zhang, *J. Hazard. Mater.*, 2025, **484**, 136724.
36 H. Bian, B. Ma, G. Yu, F. Dong, Y. Li, Y. Xu and H. Tan, *Food Res. Int.*, 2024, **196**, 115010.
37 J. Peng, J. Zhang, L. Han, X. Ma, X. Hu, T. Lin, L. He, X. Yi, J. Tian and M. Chen, *J. Food Compos. Anal.*, 2024, **135**, 106635.
38 Y. Cao, J. Sun, K. Yao, M. Xu, N. Tang and X. Zhou, *J. Food Process Eng.*, 2021, **44**, e13793.
39 X. Zhou, J. Sun, Y. Tian, B. Lu, Y. Hang and Q. Chen, *Food Chem.*, 2020, **321**, 126503.
40 J. Sun, Y. Cao, X. Zhou, M. Wu, Y. Sun and Y. Hu, *J. Food Saf.*, 2021, **41**, e12866.
41 C. Sunli, S. Jun, M. Hanping, W. Xiaohong, W. Pei and Z. Xiaodong, *J. Sci. Food Agric.*, 2018, **98**, 1453–1459.
42 X. Zhang, Y. Wang, Z. Zhou, Y. Zhang and X. Wang, *Foods*, 2023, **12**(3), 535.
43 Y.-K. Kim, I. Baek, K.-M. Lee, G. Kim, S. Kim, S.-Y. Kim, D. Chan, T. J. Herrman, N. Kim and M. S. Kim, *Toxins*, 2023, **15**, 472.
44 I. Teixido-Orries, F. Molino, F. Gatius, V. Sanchis and S. Marín, *Food Control*, 2023, **153**, 109952.
45 Y. Wang, X. Ou, H.-J. He and M. Kamruzzaman, *Food Chem.:X*, 2024, **21**, 101235.
46 H. Chen, J. Wang, W. Zhang, Y. Li, X. Zhang, X. Huang, Y. Shi, Y. Zou, Z. Li, J. Shi and X. Zou, *J. Food Compos. Anal.*, 2025, **140**, 107266.
47 X. Zhang, Y. Zhou, J. Wang, X. Huang, H. S. El-Mesery, Y. Shi, Y. Zou, Z. Li, Y. Li, J. Shi and X. Zou, *Food Chem.*, 2025, **467**, 142342.
48 X. Zhang, Y. Zhou, H. Wang, X. Huang, Y. Shi, Y. Zou, X. Hu, Z. Li, J. Shi and X. Zou, *Anal. Chim. Acta*, 2024, **1304**, 342515.
49 L. Ding, J. Guo, S. Chen and Y. Wang, *Talanta*, 2024, **273**, 125937.
50 K. Wang, X. Lin, M. Zhang, Y. Li, C. Luo and J. Wu, *Biosensors*, 2022, **12**, 959.
51 F. You, Z. Wen, R. Yuan, J. Qian, L. Long and K. Wang, *Food Chem.*, 2023, **403**, 134397.
52 Y. Xu, W. Zhang, J. Shi, Z. Li, X. Huang, X. Zou, W. Tan, X. Zhang, X. Hu, X. Wang and C. Liu, *Food Chem.*, 2020, **322**, 126762.
53 Z. Liu, L. Wang, P. Liu, K. Zhao, S. Ye and G. Liang, *Food Chem.*, 2021, **357**, 129753.
54 X. Wang, Y. Xu, Y. Li, Y. Li, Z. Li, W. Zhang, X. Zou, J. Shi, X. Huang, C. Liu and W. Li, *Food Chem.*, 2021, **357**, 129762.
55 J. Liu, L. Geng, H. Wang, J. Huang, G. Wang, Z. Shen, M. Hu, B. Li, J. Sun, J. Dong, Y. Guo and X. Sun, *Sens. Actuators, B*, 2024, **410**, 135665.
56 X. Zhang, Z. Wang, X. Li, W. Xiao, X. Zou, Q. Huang and L. Zhou, *Analyst*, 2023, **148**, 912–918.
57 H. Shu, T. Lai, Z. Yang, X. Xiao, X. Chen and Y. Wang, *Food Chem.*, 2023, **408**, 135221.
58 G. Kaur, S. Sharma, S. Singh, N. Bhardwaj and A. Deep, *ACS Omega*, 2022, **7**, 17600–17608.
59 S. Liu, S. Meng, M. Wang, W. Li, N. Dong, D. Liu, Y. Li and T. You, *Food Chem.*, 2023, **410**, 135450.
60 Y. Jiang, Y. Sima, L. Liu, C. Zhou, S. Shi, K. Wan, A. Chen, N. Tang, Q. He and J. Liu, *Chem. Eng. J.*, 2024, **485**, 149860.
61 S. Hormozi Jangi and A. Khoobi, *Food Chem.*, 2024, **458**, 140307.
62 W. Zhang, Y. Xu and X. Zou, *Food Chem.*, 2018, **261**, 1–7.
63 Z.-H. Xu, X. Weng, S.-S. Wang, Z.-H. Huang, W. Xu, W. Xu, Y. Lin and H. Gao, *Food Chem.*, 2024, 142661.
64 X. Zhang, C. Huang, Y. Jiang, Y. Jiang, J. Shen and E. Han, *J. Agric. Food Chem.*, 2018, **66**, 10106–10112.
65 X. Huang, C. Huang, L. Zhou, G. Hou, J. Sun, X. Zhang and X. Zou, *Anal. Chim. Acta*, 2023, **1278**, 341752.
66 W. Lu, X. Dai, R. Yang, Z. Liu, H. Chen, Y. Zhang and X. Zhang, *Food Control*, 2025, **169**, 111006.
67 X. Du, W. Du, J. Sun and D. Jiang, *Food Chem.*, 2022, **385**, 132731.
68 Y. Zhao, Y. Ma, R. Zhou, Y. He, Y. Wu, Y. Yi and G. Zhu, *Food Measure*, 2022, **16**, 2596–2603.
69 W. S. Devi, R. Kaur, A. Sharma, S. Thakur, S. K. Mehta, V. Raja and F. S. Ataya, *Biosens. Bioelectron.*, 2025, **267**, 116808.
70 Md. A. Rashed, M. Faisal, S. A. Alsareii, M. Alsaiari, M. Jalalah and F. A. Harraz, *J. Environ. Chem. Eng.*, 2022, **10**, 108364.

71 C. Quintelas, E. C. Ferreira, J. A. Lopes and C. Sousa, *Biotechnol. J.*, 2018, **13**, 1700449.
72 C. Liu, R. Zou and F. Mo, *Anal. Chem.*, 2024, **96**, 15550–15562.
73 E. Shawky, L. Nahar, S. M. Nassief, S. D. Sarker and R. S. Ibrahim, *Trends Food Sci. Technol.*, 2024, **148**, 104522.
74 A. L. B. Brito, I. F. Cardoso, L. P. Viegas and R. Fausto, *Spectrochim. Acta Mol. Biomol. Spectrosc.*, 2025, **326**, 125225.
75 J. Deng, H. Jiang and Q. Chen, *Food Chem.*, 2025, **469**, 142590.
76 G. Shen, X. Kang, J. Su, J. Qiu, X. Liu, J. Xu, J. Shi and S. R. Mohamed, *Food Chem.*, 2022, **384**, 132487.
77 Y.-H. Yun, H.-D. Li, B.-C. Deng and D.-S. Cao, *Trac. Trends Anal. Chem.*, 2019, **113**, 102–115.
78 Z. Guo, M. Wang, A. A. Agyekum, J. Wu, Q. Chen, M. Zuo, H. R. El-Seedi, F. Tao, J. Shi, Q. Ouyang and X. Zou, *J. Food Eng.*, 2020, **279**, 109955.
79 K. Yao, J. Sun, J. Cheng, M. Xu, C. Chen and X. Zhou, *J. Food Process Eng.*, 2023, **46**, e14186.
80 Y. Rong, M. Zareef, L. Liu, Z. U. Din, Q. Chen and Q. Ouyang, *Meat Sci.*, 2023, **201**, 109170.
81 J. Sun, A. Nirere, K. D. Dusabe, Z. Yuhao and G. Adrien, *J. Food Sci.*, 2024, **89**, 4403–4418.
82 N. Yang, M. Yuan, P. Wang, R. Zhang, J. Sun and H. Mao, *J. Sci. Food Agric.*, 2019, **99**, 3459–3466.
83 C. Yang, D. Duan, C. Dong, C. Li, G. Li, Y. Zhou, Y. Gu, Y. Liu, C. Zhao and D. Dong, *Food Chem.*, 2023, **423**, 136308.
84 Z. Wang, W. Huang, J. Li, S. Liu and S. Fan, *Comput. Electron. Agric.*, 2023, **211**, 107969.
85 H. Jiang, H. Lin, J. Lin, S. Yao-Say Solomon Adade, Q. Chen, Z. Xue and C. Chan, *Food Control*, 2022, **133**, 108640.
86 S.-Y. Zheng, Z.-S. Wei, S. Li, S.-J. Zhang, C.-F. Xie, D.-S. Yao and D.-L. Liu, *Food Chem.*, 2020, **332**, 127419.
87 H. Lin, W. Kang, E. Han and Q. Chen, *Food Chem.*, 2021, **354**, 129545.
88 Y. Zhao, J. Deng, Q. Chen and H. Jiang, *Food Chem.:X*, 2024, **22**, 101322.
89 M. B. Almoujahed, A. K. Rangarajan, R. L. Whetton, D. Vincke, D. Eylenbosch, P. Vermeulen and A. M. Mouazen, *Chemom. Intell. Lab. Syst.*, 2024, **245**, 105050.
90 Y. Zhou, L. Jiao, J. Wu, Y. Zhang, Q. Zhu and D. Dong, *Food Chem.*, 2023, **422**, 136189.
91 Q. Han, J. Lu, J. Zhu, L. Lin, Z. Zheng and S. Jiang, *Food Control*, 2025, **168**, 110858.
92 J. Zhou, X. Wu, Z. Chen, J. You and S. Xiong, *LWT*, 2019, **106**, 145–150.
93 Q. Ouyang, L. Liu, M. Zareef, L. Wang and Q. Chen, *LWT*, 2022, **160**, 113304.
94 T. Leng, F. Li, Y. Chen, L. Tang, J. Xie and Q. Yu, *Meat Sci.*, 2021, **180**, 108559.
95 E. T. D. S. Carames, K. C. Piacentini, N. Aparecida Almeida, V. Lopes Pereira, J. Azevedo Lima Pallone and L. De Oliveira Rocha, *Food Res. Int.*, 2022, **161**, 111759.
96 S. Yao, J. Fountain, G. Miyagusuku-Cruzado, M. West, V. Nwosu, E. Dowd, M. M. Giusti and L. E. Rodriguez-Saona, *LWT*, 2025, **215**, 117186.
97 H. Lin, H. Jiang, P. He, S. A. Haruna, Q. Chen, Z. Xue, C. Chan and S. Ali, *Sens. Actuators, B*, 2021, **335**, 129716.
98 X. Miao, Y. Miao, H. Gong, S. Tao, Z. Chen, J. Wang, Y. Chen and Y. Chen, *Spectrochim. Acta Mol. Biomol. Spectrosc.*, 2021, **257**, 119700.
99 A. Yazici, G. Y. Tiryaki and H. Ayvaz, *J. Sci. Food Agric.*, 2020, **100**, 1980–1989.
100 Y. Lu, X. Li, W. Li, T. Shen, Z. He, M. Zhang, H. Zhang, Y. Sun and F. Liu, *Spectrochim. Acta Mol. Biomol. Spectrosc.*, 2021, **257**, 119759.
101 F. Rodriguez-Macadaeg, P. R. Armstrong, E. B. Maghirang, E. D. Scully, D. L. Brabec, F. H. Arthur, A. D. Adviento-Borbe, K. F. Yaptenco and D. C. Suministrado, *Sensors*, 2024, **24**, 4055.
102 Y. Cui, K. Chang, Q. Wang and Y. Zhao, *Coord. Chem. Rev.*, 2025, **524**, 216320.
103 K. Chang, Y. Zhao, M. Wang, Z. Xu, L. Zhu, L. Xu and Q. Wang, *Chem. Eng. J.*, 2023, **459**, 141539.
104 Y. Xu, M. M. Hassan, S. Ali, H. Li, Q. Ouyang and Q. Chen, *J. Agric. Food Chem.*, 2021, **69**, 1667–1674.
105 L. Guo, J. Zhang, Y. Bao, Y. Zhang, D. Zhang, X. Ma and J. Zhang, *Food Chem.*, 2024, **458**, 140231.
106 P. He, M. Mehedi Hassan, W. Yang, Z. Shi, X. Zhou, Y. Xu, Q. Ouyang and Q. Chen, *Food Chem.*, 2023, **398**, 133883.
107 R. Chen, H. Wang, C. Sun, Y. Zhao, Y. He, M. S. Nisar, W. Wei, H. Kang, X. Xie, C. Du, Q. Luo, L. Yang, X. Tang and B. Xiong, *Talanta*, 2023, **258**, 124401.
108 Y. Xu, Z. Jin and Y. Zhao, *J. Agric. Food Chem.*, 2023, **71**, 1224–1233.
109 Z. Guo, L. Gao, L. Yin, M. Arslan, H. R. El-Seedi and X. Zou, *Food Chem.*, 2023, **403**, 134384.
110 L. Yin, T. You, H. R. El-Seedi, I. M. El-Garawani, Z. Guo, X. Zou and J. Cai, *Food Chem.*, 2022, **396**, 133707.
111 J. Zhu, X. Jiang, Y. Rong, W. Wei, S. Wu, T. Jiao and Q. Chen, *Food Chem.*, 2023, **414**, 135705.
112 S. Xue, L. Yin, S. Gao, R. Zhou, Y. Zhang, H. Jayan, H. R. El-Seedi, X. Zou and Z. Guo, *Food Chem.*, 2024, **441**, 138364.
113 Z. Guo, P. Chen, M. Wang, M. Zuo, H. R. El-Seedi, Q. Chen, J. Shi and X. Zou, *LWT*, 2021, **152**, 112333.
114 H. Li, W. Geng, M. M. Hassan, M. Zuo, W. Wei, X. Wu, Q. Ouyang and Q. Chen, *Food Control*, 2021, **128**, 108186.
115 X. Wu, L. Yin, S. Gao, R. Zhou, Y. Zhang, S. Xue, H. Jayan, H. R. El-Seedi, X. Zou and Z. Guo, *Food Control*, 2024, **159**, 110293.
116 J. H. Aheto, X. Huang, X. Tian, X. Zhang, W. Zhang and S. Yu, *J. Food Saf.*, 2023, **43**, e13072.
117 H. Li, M. M. Hassan, Z. He, S. A. Haruna, Q. Chen and Z. Ding, *LWT*, 2022, **167**, 113804.
118 L. Ma, E. Han, L. Yin, Q. Xu, C. Zou, J. Bai, W. Wu and J. Cai, *Food Control*, 2023, **153**, 109951.
119 F. Bai, J. Dong, T. Wang, J. Qu and Z. Zhang, *Food Chem.*, 2023, **405**, 134794.
120 H. Pan, W. Ahmad, T. Jiao, A. Zhu, Q. Ouyang and Q. Chen, *Food Chem.*, 2022, **375**, 131681.
121 Y. Sun, X. Zhai, Y. Xu, C. Liu, X. Zou, Z. Li, J. Shi and X. Huang, *Food Control*, 2021, **122**, 107772.

122 X. Wei, W. Song, Y. Fan, Y. Sun, Z. Li, S. Chen, J. Shi, D. Zhang, X. Zou and X. Xu, *Food Chem.*, 2024, **431**, 137120.
123 X. Huang, N. Zhang, Z. Li, J. Shi, H. Tahir, Y. Sun, Y. Zhang, X. Zhang, M. Holmes and X. Zou, *Foods*, 2022, **11**, 1287.
124 Y. Liu, R. Xue and B. Yan, *Coord. Chem. Rev.*, 2025, **523**, 216280.
125 N. Liang, X. Hu, W. Li, Y. Wang, Z. Guo, X. Huang, Z. Li, X. Zhang, J. Zhang, J. Xiao, X. Zou and J. Shi, *Food Chem.*, 2022, **378**, 132076.
126 C. Zhang, Y. Han, L. Lin, N. Deng, B. Chen and Y. Liu, *J. Agric. Food Chem.*, 2017, **65**, 1290–1295.
127 S. Yadav, N. Choudhary and A. R. Paital, *Carbon*, 2023, **205**, 527–539.
128 W. Pervez, Laraib, C. Yin and F. Huo, *Coord. Chem. Rev.*, 2025, **522**, 216202.
129 L. Guan, Y. Zhou, X. Li, Y. Mao, A. Li, Y. Fu, W. Liu, S. Dong, Z. Liang, Y. Zhang, Q. Zhao and L. Zhang, *Anal. Chem.*, 2023, **95**, 9288–9296.
130 D. K. Mal, H. Pal and G. Chakraborty, *Trac. Trends Anal. Chem.*, 2024, **171**, 117493.
131 X. Huang, W. Sun, Z. Li, J. Shi, N. Zhang, Y. Zhang, X. Zhai, X. Hu and X. Zou, *Food Chem.*, 2022, **396**, 133654.
132 Y. Hu, S. Guo, J. Peng, Y. Fan, F. Wang, L. Lu, H. Fu, X. Chen and Y. She, *Sens. Actuators, B*, 2023, **392**, 134064.
133 Z. Gan, W. Zhang, M. Arslan, X. Hu, X. Zhang, Z. Li, J. Shi and X. Zou, *J. Agric. Food Chem.*, 2022, **70**, 10065–10074.
134 H. Qiu, L. Gao, J. Wang, J. Pan, Y. Yan and X. Zhang, *Food Chem.*, 2017, **217**, 620–627.
135 Q. Li, J. Wu, Q. Yang, H. Li and F. Li, *Anal. Chem.*, 2021, **93**, 7362–7368.
136 C. Zhang, H. Cui, J. Cai, Y. Duan and Y. Liu, *J. Agric. Food Chem.*, 2015, **63**, 4966–4972.
137 Q. Ouyang, L. Wang, W. Ahmad, Y. Rong, H. Li, Y. Hu and Q. Chen, *Food Chem.*, 2021, **349**, 129157.
138 L. Wang, S. A. Haruna, W. Ahmad, J. Wu, Q. Chen and Q. Ouyang, *Food Chem.*, 2022, **388**, 132950.
139 W. Li, X. Hu, Q. Li, Y. Shi, X. Zhai, Y. Xu, Z. Li, X. Huang, X. Wang, J. Shi, X. Zou and S. Kang, *Food Chem.*, 2020, **320**, 126623.
140 S. Hassibian, M. Esmaelpourfarkhani, K. Abnous, M. Amin, F. Ghazvinian, M. Alibolandi, M. Ramezani, M. A. Nameghi, H. Mollasalehi, N. Farrokhi, S. M. Dehnavi and S. M. Taghdisi, *Food Chem.*, 2025, **463**, 141440.
141 Y. Zhou, G. Chen, C. Ma, J. Gu, T. Yang, L. Li, H. Gao, Y. Xiong, C. Zhu, A. Hu, X. Li, W. Guan and W. Zhang, *Dyes Pigm.*, 2024, **222**, 111845.
142 L. Li, S. Xu, X. Li, H. Gao, L. Yang and C. Jiang, *Chem. Eng. J.*, 2024, **493**, 152636.
143 X. Wang, H. Yu, Q. Li, Y. Tian, X. Gao, W. Zhang, Z. Sun, Y. Mou, X. Sun, Y. Guo and F. Li, *Food Chem.*, 2024, **431**, 137067.
144 X. Dou, G. Wu, Z. Ding and J. Xie, *Food Chem.*, 2023, **416**, 135805.
145 L. Sun, X. Zheng, H. Yang, Y. Zhu, J. Zhang, X. Zhang and Y. Zhou, *Microchem. J.*, 2024, **206**, 111427.
146 X. Bi, L. Li, X. Liu, L. Luo, Z. Cheng, J. Sun, Z. Cai, J. Liu and T. You, *Food Chem.*, 2021, **349**, 129171.
147 K. Majer-Baranyi, A. Barocsi, P. Gadoros, L. Kocsanyi, A. Szekacs and N. Adanyi, *Toxins*, 2022, **14**, 866.